NTRD
Technical Monthly
September FY17

Nuclear Technology
Research and Development

Prepared for
U.S. Department of Energy

November 21, 2017

NTRD-PAC-2017-000440
INL/EXT-17-43850

CONTENTS

FIGURES

ADVANCED FUELS CAMPAIGN

MATERIAL RECOVERY AND WASTE FORMS DEVELOPMENT

NUCLEAR TECHNOLOGY RESEARCH AND DEVELOPMENT TECHNICAL MONTHLY SEPTEMBER FY17

ADVANCED FUELS CAMPAIGN

INTERNATIONAL COLLABORATIONS

- K. McClellan and E. Kardoulaki participated in technical meetings in the UK (University of Manchester) and Germany (JRC-Karlsruhe) to coordinate activities under the US/Euratom I-NERI project titled "Field assisted sintering studies in support of nuclear fuel safety test specimen development and analysis." LANL, RPI, BNL and INL are I-NERI participants on the US side while participants on the Euratom side include JRC-Karlsruhe, Karlsruhe Institute of Technology (KIT), University of Manchester and the UK's National Nuclear Laboratory. Status of studies at LANL as well as joint LANL/RPI and LANL/BNL studies were presented under the US contribution and in turn, updates were presented by each of the Euratom participants. Discussions with partners from JRC and KIT have led to planning collaborative experiments to showcase O/M and grain size variations in UO_2 pellets due to a field effect. Discussions were also initiated on collaborative *in-situ* studies that could be done at facilities such as BNL's NSLS-II. (K. McClellan)

ADVANCED LWR FUELS

LWR Computational Analysis

Metrics Development for ATF

- **[INL]** S. Bragg-Sitton and B. Merrill held a teleconference on August 22 with researchers from General Atomics (GA) to discuss the possible use of the modified version of MELCOR for analysis of ATF. GA is interested in having INL extend the MELCOR work led by B. Merrill to update the SiC failure modes per their current data/understanding and to add U3Si2 fuel to the materials options. GA may also want to link FRAPTRAN with MELCOR. The discussion focused on feasibility, given GA provides the fuel data and SiC failure models. A follow-on discussion was held with GA management on Friday, September 8 to address timeline and funding for the proposed work. No decision was made regarding final path forward. (S. Bragg-Sitton)
- **[INL]** The OECD/NEA EGATFL deliverable report on systems assessment was completed, incorporating all recommended edits and comments from the international members of the task force. The document was submitted to NEA for final formatting and editing on September 26. A final meeting of the OECD/NEA EGATFL is scheduled November 2-3 at NEA Headquarters in Paris to obtain final approval on the Systems Assessment Task Force (EGATFL Task Force 1) report and the State-of-the-Art reports on Accident Tolerant Fuel and Cladding, produced by EGATFL Task Forces 2 and 3. (S. Bragg-Sitton)
- **[INL]** Milestone M3FT-17IN020205021, Status report on NEA ATF Expert Group progress within the "Systems Assessment" task force, was completed on 9/28/2017. This report summarizes the content included in the overall task force report submitted to NEA. (S. Bragg-Sitton)

Analyses

- **[BNL]** The analysis of a station blackout (SBO) continued with a variant scenario. A "bottled" up reactor was analyzed previously resulting in a system pressurization that exceeded the critical pressure (22.06 MPa) in about 95 sec. That TRACE run terminated shortly after the reactor pressure exceeded the critical pressure due to thermal property issues. A modified SBO scenario was analyzed. The new case allowed the pressurizer safety relief valve (SRV) to actuate, leading to a situation similar to a small-break loss-of-coolant accident (SBLOCA). In this new case the reactor pressure (see Figure 1) was seen being modulated within the operating band of the pressurizer SRV. The corresponding core coolant temperature (see Figure 2) reached saturation condition in about 1000 sec. after the initiation of the SBO accident. In the case of a SBO with a "bottled" up reactor, the timing of the loss of cooling is rather uncertain because of potential random leakages from primary components before catastrophic failures due to pressurization. In the case of the modified SBO scenario, the opening of the pressurizer SRV leads to loss of coolant from the reactor that can be calculated analytically. (L.-Y. Cheng)

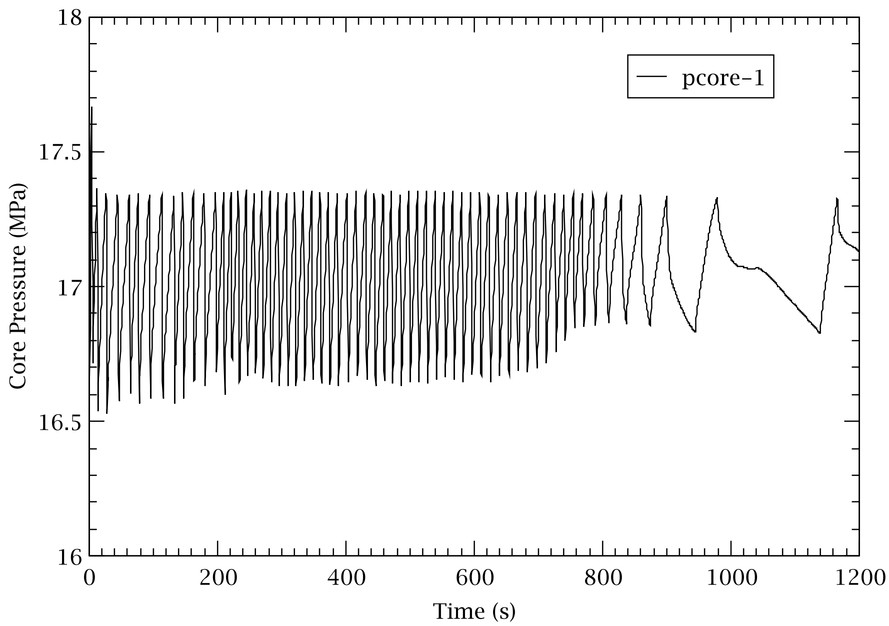

Figure 1. Core pressure.

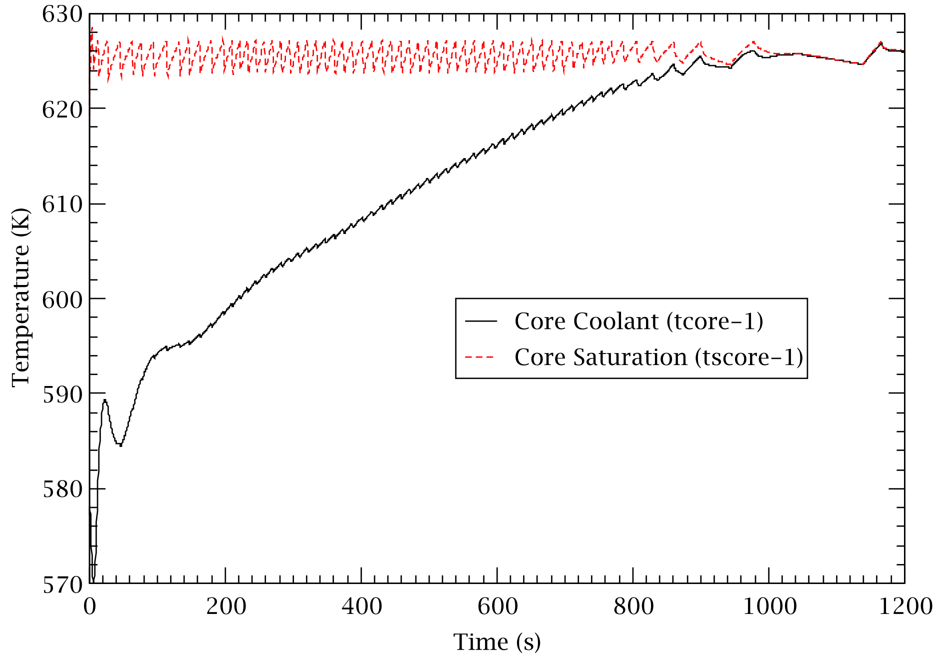

Figure 2. Core coolant temperature.

LWR Fuels

- **[LANL]** The M2 milestone M2FT-17LA020201031, "Development of strategies to relax handling constraints for high density fuels," was completed. The report describes efforts to mitigate the surface oxidation that is detrimental to the sintering of high uranium density fuels. Techniques developed in this study allow the handling of green pellets of U_3Si_2 in air without pyrophoric reactions and allow densities >89% after sintering, which can also be potentially applied to other high uranium density fuels. One of the identified issues with high density fuels is that the powders readily oxidize even when low oxygen levels are present which leads to decreased sinterability in the powders. Research has been conducted on the ageing of U_3Si_2 and UN powders in both a glove box and ambient air conditions. The U_3Si_2 powders gained approximately 4000 wppm O in both environments although at a much-accelerated rate in air, while the UN powders rapidly oxidized in air and gained 5700 wppm oxygen in the glove box over the course of 18 days and trending to increase further. A high binder loading system with 30 vol% (3.45 wt%) binder was developed using systematic studies on UO_2 and U_3Si_2. Microscopy studies were utilized to develop strategies to improve upon the distribution of polymeric additives in the fuel matrix using a combination of mixing, milling, heating, and sieving the fuel/binder system, which improved the final density of the sintered product to densities greater than 90% of theoretical density. Efficient methods were also developed in a TGA to thermally debind the polymer from the fuel matrix in an Ar or in a vacuum environment, generally totaling less than 62 hours of total debinding and sintering time in a furnace. Experiments were also conducted on the properties of U_3Si_2 that were sintered under more standard binder loadings (0.25 wt%) but sintered using different atmospheres of Ar(g), 6%H_2/Ar, or vacuum. Each of the measurements showed similar thermal diffusivity values on heating to 1000°C, but the hydrogen sintered specimen deviated to lower values on cooling below 400°C. It is believed that the deviation in thermal diffusivity values while cooling in the hydrogen sample is a result of exsolution of hydrogen from the U_3Si_2 lattice to form a low temperature U-Si-H phase, but further work is required to understand the origins of this phenomenon. (J. White)

- **[LANL]** The M3 milestone M3FT-17LA020201038, "Development of High Density Fissile Composites," was completed. The report summarizes work accomplished to date in developing and refining high density fuel compositions. Uranium mononitride (UN) is a strong candidate for inclusion as a constituent in LWR fuels. However, its poor oxidation behavior represents a significant liability. Here, composite materials consisting of a UN secondary phase blended into a UO_2 primary phase have been synthesized. The microstructure, thermal diffusivity, and oxidation behavior have been analyzed. The composite materials have been found to have an increase in thermal conductivity but exhibit a decrease in oxidation behavior, when compared to UO_2. This work represents a major milestone from a fuel fabrication standpoint as this is the first time UO_2/UN composites have been synthesized to better than 90% theoretical density without the aid of pressure (e.g. hot pressing) or current (e.g. spark plasma sintering). The developments here lay the groundwork for planned FY18 work to assess whether UO_2 is capable of shielding UN or any secondary fissile phase from degradation under oxidizing atmospheres. (N. Wozniak)
- **[LANL]** The M3 milestone M3FT-17LA020201037, "Update on Mechanical Properties of U-Si High Density LWR Fuels," was completed. In this report, the elastic properties of U_3Si_2 at room temperature have been measured via Resonant Ultrasound Spectroscopy. The Resonant Ultrasound Spectroscopy test results show that the measured average value of Young's and the Bulk modulus for U_3Si_2 is 130.4±0.5 and 68.3±0.5 GPa, respectively. Furthermore, various mechanical testing methods were used to examine the mechanical properties of U_3Si_2 in comparison with U_3Si and USi as a permissible impurities phase content. The Young's Modulus value of the U_3Si_2 and U_3Si analyzed from nanoindentation loading curves was 155±3 and 134 ±5 GPa, respectively. A reduced modulus of 157±3 GPa was obtained for USi. Hardness of 11.9±0.04 GPa, 6.4±0.3 GPa and 13.8±0.2 GPa was achieved for U_3Si_2, U_3Si and USi from the analysis using the unloading curves. In addition, microindentations was used to evaluate the mechanical properties varying the composition U_3Si shows the lowest value of hardness at 282±14 Hv, following by U_3Si_2 with a value of hardness at 462±37 Hv. USi exhibits the greatest hardness at 508±58 GPa. These results will be expanded to elevated temperatures in FY18. (U. Carvajal-Nunez)
- **[LANL]** The M2 milestone: M2FT-17LA020201041 "Separate Effects Study of Oxygen on Fresh Fuel Properties of U_3Si_2," was completed. The report describes efforts to investigate the effects of oxygen on thermophysical and microstructural properties of U_3Si_2 using a separate effects approach to fuel development. A number of factors (e.g. feedstock synthesis, storage, air exposure, sintering environment) have been found capable of increasing the oxygen content in U_3Si_2 feedstock. This research aims to determine the impact, if any, of oxygen incorporated as UO_2 on the thermal conductivity of U_3Si_2. A 'composite materials' approach was utilized to fabricate specimens with varying amounts of UO_2 within the U_3Si_2 matrix. The microstructure and density of sintered composites were analyzed in reference to standard U_3Si_2 behavior. Laser flash analysis was used to determine thermal diffusivity of the composites to assess whether oxygen addition of these levels would be expected to degrade the thermal conductivity of U_3Si_2. Oxygen contents approximately equal to 2, 4, 6, 8, and 10 vol. % UO_2 were incorporated in a traditional U_3Si_2 pellet fabrication process. Thermal diffusivity data was collected on these samples from room temperature to 600° C and compared to those of pure U_3Si_2. The addition of oxygen degraded the density of samples and resulted in perturbations to the resulting microstructure as expected based on previous experience. However, even these extreme impurity levels and microstructural distortions did not drastically degrade thermal transport. The most extreme reduction in thermal conductivity was found to be approximately ten percent below that of pure U_3Si_2 at fuel operating temperatures. This magnitude of

reduction can be considered a bounding case when considering potential implications of oxygen uptake on large scale fabrication of U_3Si_2 (J. Dunwoody).

- **[ORNL]** A presentation was given at the 40th Enlarged Halden Programme Group Meeting in Lillehammer, Norway on a new irradiation testing capability at ORNL. This new capability allows for irradiation of miniature fuel specimens in small sealed sub-capsules in the reflector positions of the High Flux Isotope Reactor. The small size of the fuel specimens greatly simplifies the design, analysis, and post-irradiation examination. In theory, any fuel (e.g., varying composition, enrichment, and, to some extent, geometry) can be irradiated in this configuration provided that the total fuel heat load is within the safety basis established for this experiment. This flexibility in the design will help provide basic scientific data on the irradiation performance of a wide variety of advanced fuel concepts with significantly reduced cost. (C. Petrie, K. Terrani)
- **[INL]** Westinghouse 00001063 FOA Grinding for all enriched U3Si2 pellets required for the ATF-2 experiment was completed. (G. Core)
- **[INL]** Forty-six enriched pellets were shipped to General Atomics on 9/28/17, meeting the originally agreed upon deadline of 9/30/17. (G. Core)

LWR Core Materials

Thin Walled Tube Development

- **[INL]** Samples 38-13 – 38-16, bonded using the PRW, were analyzed using x-ray CT to visualize the developed bond. Samples 38-13 & 14 were bonded using the r10 endplug design where samples 38-15 & 16 were bonded using the r11 endplug design. Cross-section renderings of the four samples show good axial alignment and good bond formation has occurred through the joining process. All four samples show a remarkable improvement in bond development due to the increased joining currents used (Figure 3). (J. Gan)

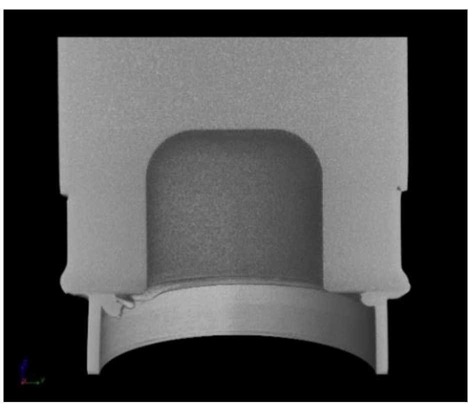

Sample 38-13

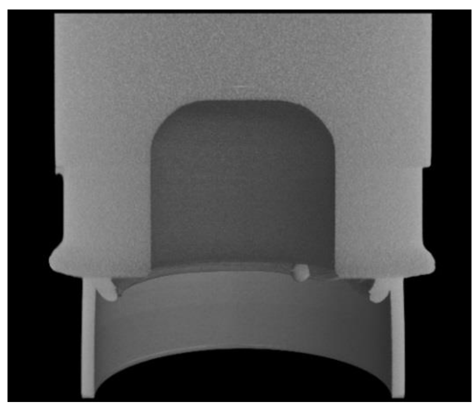

Sample 38-14

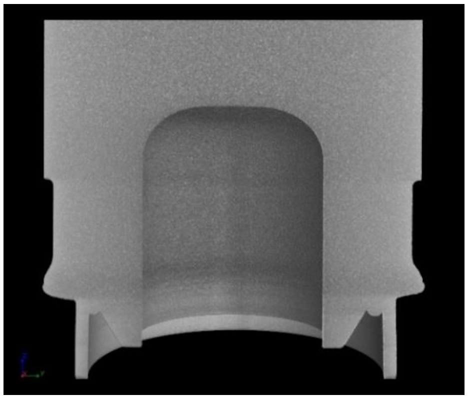

Sample 38-15

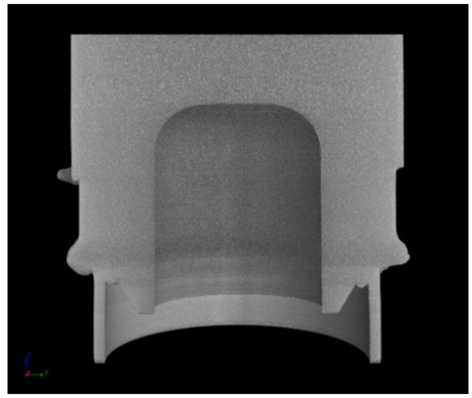

Sample 38-16

Figure 3. Samples 38-13 through 38-16.

- **[INL]** Samples 37-3 – 37-6, joined using the LBW process, were tested in the PWHT condition at elevated temperatures (Figure 4). Samples were tested at temperatures noted below. All four samples had thermocouples attached to the exterior surface to monitor sample temperature through the test and all were tested using the same fixture setup. All samples showed elongation in the tube with failure occurring in the tube. Figure 5 shows the results of the tests. NOTE: for testing all threads were coated with boron nitride to prevent bonding at elevated temperature. ***NOTE:*** sample 37-3 showed an abnormally thinned cladding wall, likely from fabrication, compared to the other tested samples, measuring ~280µm. This is believed to be the reason for sample 37-3 early failure in the tube and limited reported strain. For this reason, sample 37-5 was also tested at 400°C - to ensure accurate measurements at that temperature. It can be seen the weld strength is maintained through the elevated test temperatures, with failure occurring in the tube section for all samples. Further, it is seen both the tensile strength and yield strength decreases with testing temperature – as expected. ***NOTE:*** sample 37-4 shows a lower yield strength compared to samples 37-3 & 37-5. This may be an anomaly and additional tests at each test temperature are needed to fully understand the materials behavior. (J. Gan)

Sample 37-6

Test Temp: ~25°C

UTS: 703 MPa, Max Strain: 26.22%

YS: 551 MPa, Failure Location: TUBE

Sample 37-4

Test Temp: 300°C

UTS: 657 MPa, Max Strain: 23.12%

YS: 441 MPa, Failure Location: TUBE

Sample 37-3

Test Temp: 400°C

UTS: 548 MPa, Max Strain: 12.62%

YS: 479 MPa, Failure Location: TUBE

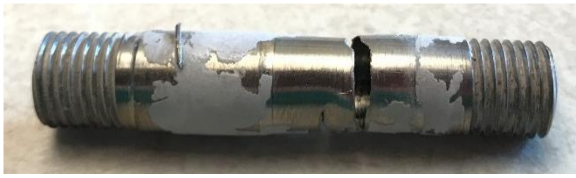

Sample 37-5

Test Temp: 400°C

UTS: 542 MPa, Max Strain: 28.13%

YS: 462 MPa, Failure Location: TUBE

Figure 4. Samples 37-3 through 37-6.

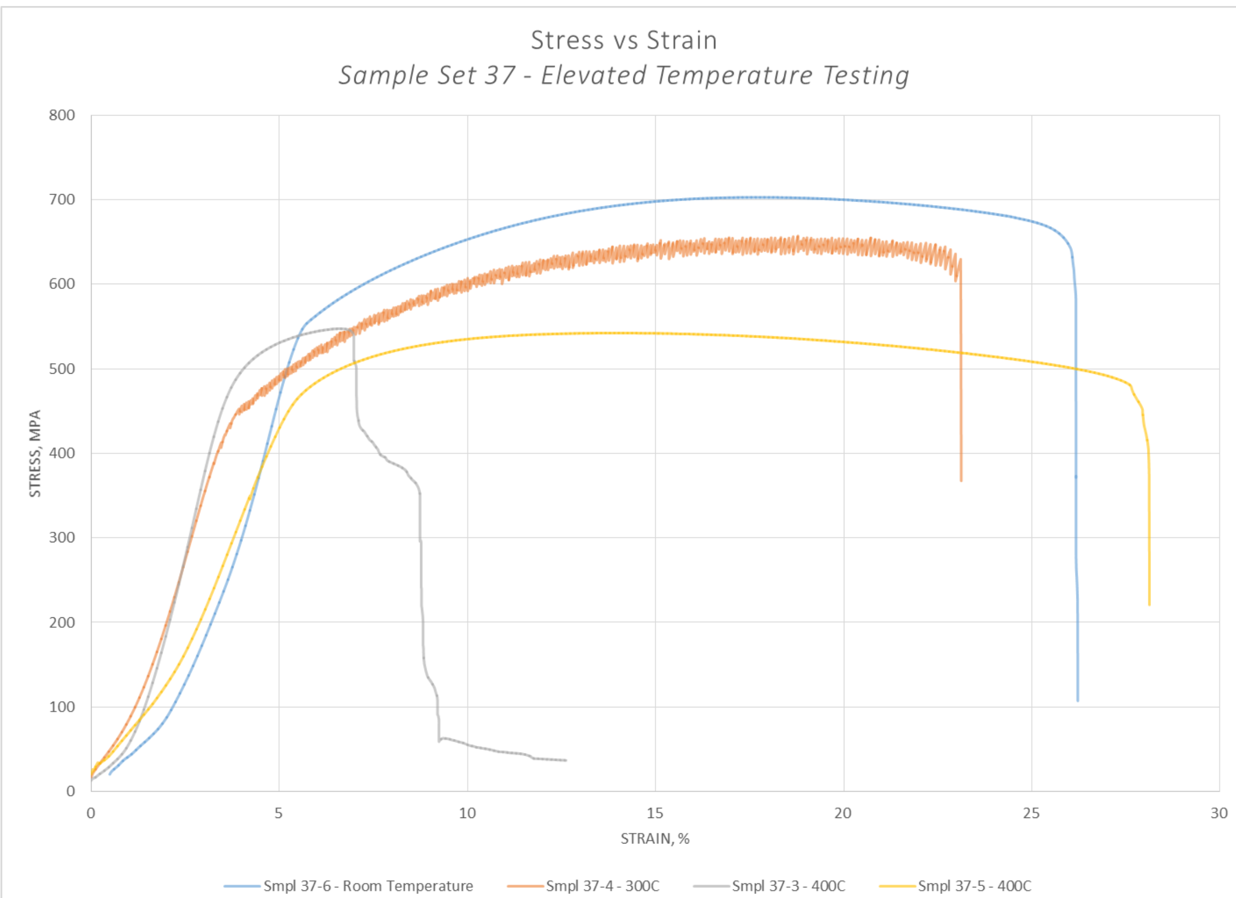

Figure 5. Sample set 37 elevated temperature testing.

- Figure 6 shows the test temperature plots recorded from the attached thermocouples for the four samples tested. Sample temperatures were kept at the test temperature ± 5° for the duration of the test.

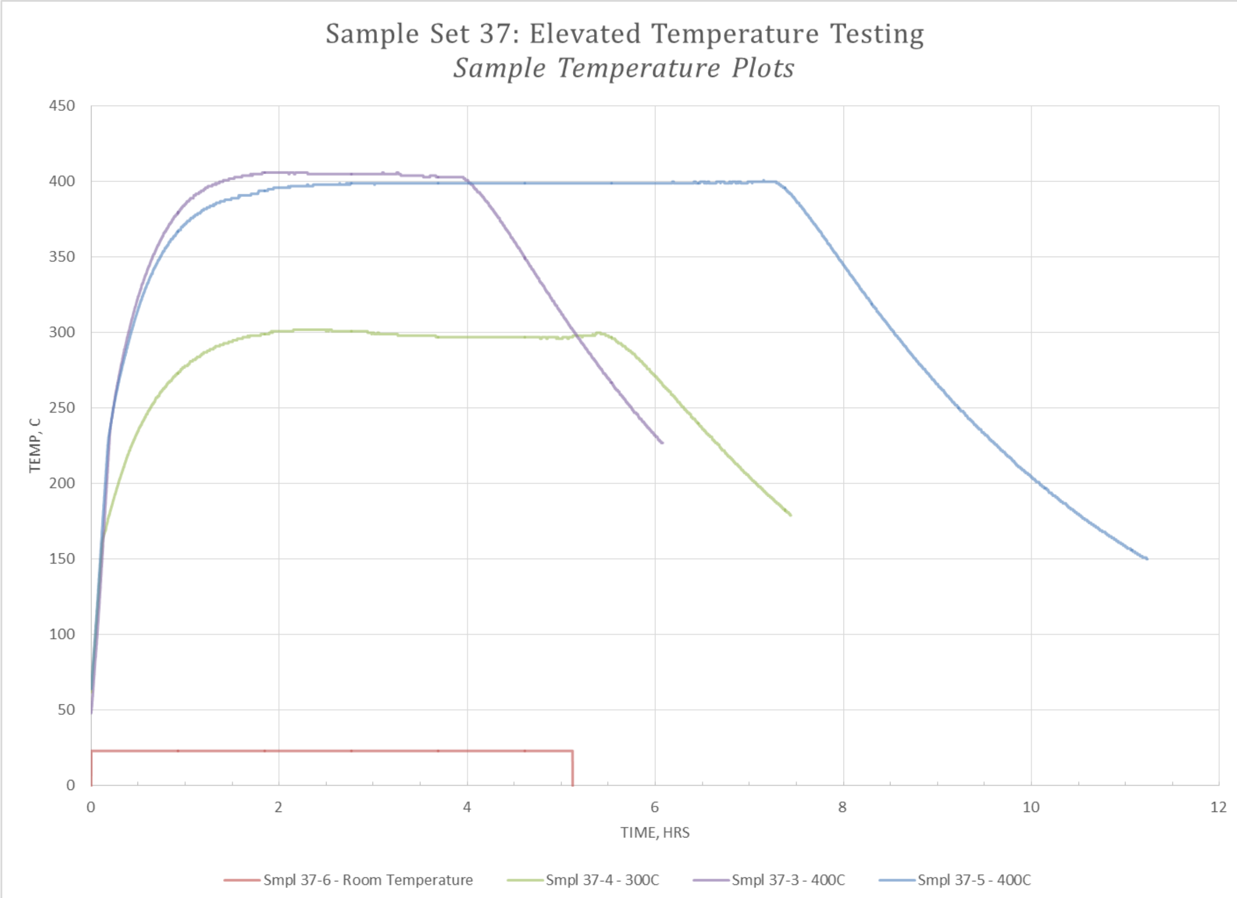

Figure 6. Test temperature plots recorded from the attached thermocouples for the four samples tested.

- **[INL]** Samples 38-11 – 38-16, bonded using the PRW process, were tensile tested in the 'as-joined' condition at room temperature to evaluate the bond strength for the various samples (Figure 7 and Figure 8). Samples 38-11 through 38-14 utilized the r10 endplug design, which has a flat bonding surface with a central hole. Samples 38-11 & 38-12 were joined using the same joining parameters, but their joining current and energy were measured to be 12.45 kA & 1133 J and 12.07 kA & 1106 J, respectively. It can be seen that at the same joining parameters, the fluctuation in joining current, and thus joining energy, is sufficient to cause a significant change in bond strength. This is seen where sample 38-11 shows a bond strength that exceeds that of the tube material where sample 38-12 shows a mixed failure in the weld & tube occurring below the material yield strength. Therefore, for samples 38-13 & 38-14, the joining parameters were changed to apply an increased joining current. Such a change resulted in measured joining currents & energies to be 12.53 kA & 1202 J and 13.58 kA & 1343 J, for samples 38-13 & 38-14 respectively. It can be seen both samples 38-13 & 38-14 showed a bond strength that exceeded that of the tube material and both exhibited favorable tensile results. ***NOTE:*** moving forward, joining parameters will be used that are favored towards that used for sample 38-14 to provide a buffer in bond strength for possible fluctuations in the joining current & energy, as was seen between samples 38-11 & 38-12. Samples 38-15 & 38-16 utilized the r11 endplug design which incorporates an internal tapered section to facilitate axial alignment between the cladding and endplug parts along with an internal hole. However, as was seen in samples 38-9 & 38-10 which also utilized the r11 endplug design, contact between the inner cladding wall was believed to have been made with the tapered section of the endplug, leading to an increase in contact area and thus a decrease in local current density. It is believed this is what led to the poor bond strength exhibited in samples 38-9 & 38-10. Therefore, samples 38-15 & 38-16 were bonded using elevated joining currents & energies measured to be 14.36 kA & 1356 J and 15.08 kA & 1606 J, respectively. As can be seen, the increased joining current did not bond well for sample 38-15 showing early failure at the weld. However, the increased joining current for sample 38-16 did facilitate a bond strength that exceeded that of the tube material undergoing failure in the tube section. ***NOTE:*** additional, testing is needed to confirm adequate joining parameters for the r11 endplug design. ***NOTE***: in evaluating the tensile curves for samples 38-11, 38-13, 38-14 & 38-16, all four samples show similar trends having tensile and yield strengths that are consistent and in good agreement with each other. (J. Gan)

Smpl 38-11

Endplug design: r10

UTS: 658 MPa, Max Strain: 18.21%

YS: 593 MPa, Failure Location: TUBE

Smpl 38-12

Endplug design: r10

UTS: 446 MPa, Max Strain: 2.00%

YS: n/a, Failure Location: WELD/TUBE

Smpl 38-13

Endplug design: r10

UTS: 694 MPa, Max Strain: 19.02%

YS: 629 MPa, Failure Location: TUBE

Smpl 38-14

Endplug design: r10

UTS: 682 MPa, Max Strain: 20.05%

YS: 603 MPa, Failure Location: TUBE

Smpl 38-15

Endplug design: r11

UTS: 516 MPa, Max Strain: 3.97%

YS: n/a, Failure Location: WELD

SAMPLE DESTROYED IN REMOVAL FROM FIXTURES

NO PICTURE AVAILABLE

Smpl 38-16

Endplug design: r11

UTS: 681 MPa, Max Strain: 26.08%

YS: 620 MPa, Failure Location: TUBE

Figure 7. Samples 38-11 through 38-16.

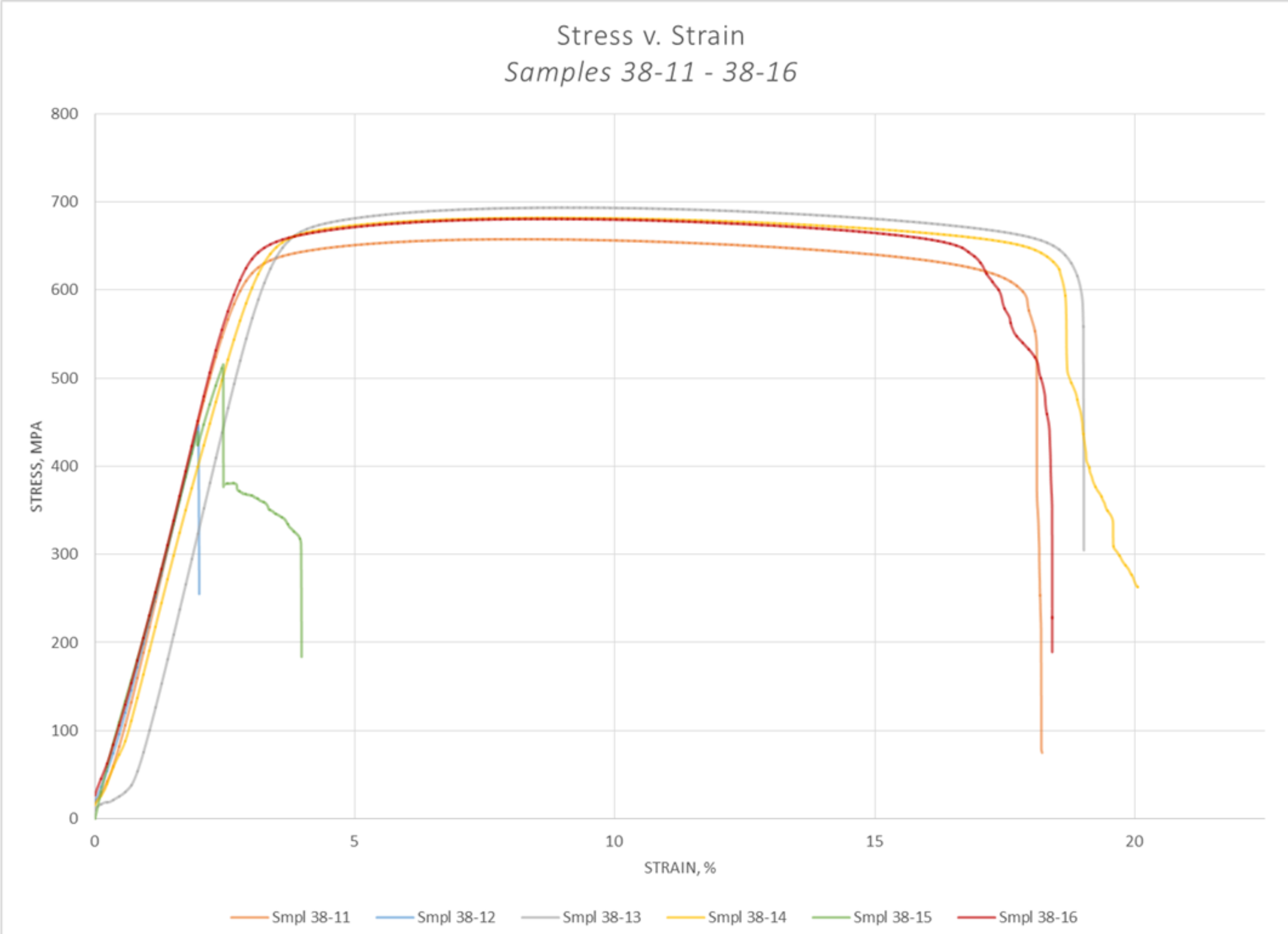

Figure 8. Samples 38-11 through 38-16 stress v. strain.

- **[INL]** Based on the favorable tensile results seen between samples 38-11, 38-13 & 38-14 and given the limited time remaining in the project, elevated temperature tensile testing of PRW bonds will be pursued using the r10 endplug design utilizing already fabricated endplugs. However, to facilitate elevated temperature testing and prevent the internal volume from pressurizing during testing, a 0.05" diameter bleed hole will be machined into the sides of the endplugs. Modification of the endplugs should be completed and ready for joining in early October. (J. Gan)

<u>Advanced LWR Materials Development and Testing</u>

- **[LANL]** Testing of HFIR irradiated FeCrAl alloys has been completed to meet the L2 milestone due in September. Data shows a strong reduction in ductility after irradiation which is in strong agreement with previous testing of FeCrAl alloys after irradiation. (T. Saleh)
- **[ORNL]** Procurement of seamless Gen II. C26M alloy tubes (Fe-12Cr-6Al-2Mo-Si-Y, wt.%) with 9.5 mm outer diameter is in progress. The inner surface quality issue observed in the first and second batch productions were summarized and shared with Century Tubes. Modified cleaning steps during the tube drawing and inter-pass annealing processes were discussed. Because of the delay to issue the PO, the expected delivery date may shift to the early 2018. (Y. Yamamoto)

- **[ORNL]** The C26M tubes and C26M2 wires were delivered GE/GNF. The products are to be used in lead test rods in Edwin I. Hatch Nuclear Power Plant, Baxley, GA, to assess the feasibility of newly developed, accident tolerant FeCrAl alloy cladding. (Y. Yamamoto)
- **[ORNL]** Additional Charpy tests of various FeCrAl alloys, made through ingot metallurgy (IM) and powder metallurgy (PM), have been completed. The data of impact absorbed energy was used to quantitatively determine the ductile-brittle transition temperature (DBTT) and the upper shelf energy of the alloys. All specimens showed typical transgranular fracture surface at room temperature and 100 °C, and the percentage of ductile fracture increased as the test temperature increased. The PM APMT alloy consisting of fine grain structure with residual strain showed predominant dimples on the fracture surface at 400 °C, although its absorbed energy value (~15 J) was significantly smaller than wrought FeCrAl alloys at 400 °C (~60 J). The same alloy with coarse grain structure had prevalent transgranular-fracture features even at 600 °C, which was consistent with its low absorbed energy (~5 J at 600 °C). Fully-annealed wrought FeCrAl alloys were ductile and did not fracture at 400 °C, whereas additional 10% warm-rolling resulted in mixed fracture surface at 400 °C. These results indicated fully annealed condition combined with grain refinement would be the key to improve the toughness of FeCrAl alloys, consistent with the conclusion reported previously. (Z. Sun, Y. Yamamoto)
- **[ORNL]** Processability evaluation of Mo/Nb-containing FeCrAl alloys is being continued to optimize the process steps and improve the quality of seamless thin-wall FeCrAl tube production. The current evaluation focuses on the intertwined effects among applied strain (10%-40%), annealing temperature (800-950 °C), and time (0.25-5 h) on microstructure evolutions and mechanical properties. These factors are to be examined, analyzed, and then used to propose the optimized process pathway for sufficient deformability during production process combined with desirable microstructures in final tube products. In parallel, the detailed characterization efforts of the Laves phase particles and element segregation along grain boundaries in Nb-containing FeCrAl alloys are currently in progress by using TEM and APT. (Z. Sun, Y. Yamamoto)
- **[LANL]** Ion irradiation was completed on two FeCrAl alloys (B136Y3 and C35M4). Irradiation was performed with Fe ions to doses up to 70 dpa. Characterization of these samples was also completed including nanohardness testing and TEM analysis. This data provides initial irradiation data on these alloys to doses up to 70 dpa. This data will be part of two L3 milestone reports on irradiation testing and nanohardness testing of FeCrAl alloys after irradiation. (S. Maloy)
- **[LANL]** Tube ring pull testing has been completed on two Generation I FeCrAl alloys to meet a L3 milestone. The data provided in this milestone provides tensile properties in the radial direction on FeCrAl tubing which can be compared to irradiation data measured on tubes also. (S. Maloy)
- **[ORNL]** The Level 3 milestone (M3FT-17OR020201072) was submitted on September 1, which described modeling to provide thermo-mechanical analysis of SiC/SiC cladding with BISON, including fuel creep. Subsequently the modeling effort focused on an initial finite element modeling assessment of the thermal mechanical performance of a SiC channel box in a BWR, based on neutronics/CFD modeling input on heat load and neutron flux. Modeling effort on evaluating the FeCrAl cladding has focused on further assessments of the influence of fuel mechanics associated with sintering, irradiation creep and fuel cracking on the gap closure and stress development in the FeCrAl cladding. (G. Singh, B. Wirth, Y. Katoh)
- **[ORNL]** Detection of micro cracks is critically important to assess SiC composite cladding because of relevance to hermeticity. During this period, we demonstrated such micro cracks within SiC composite tubes can be detected by X ray computed tomography (XCT) with a high-resolution setting. We now have this capability for evaluation of radioactive material. The XCT image shown in Figure 9 below shows micro cracks in neutron irradiated SiC tube. (T.Koyanagi, Y.Katoh)

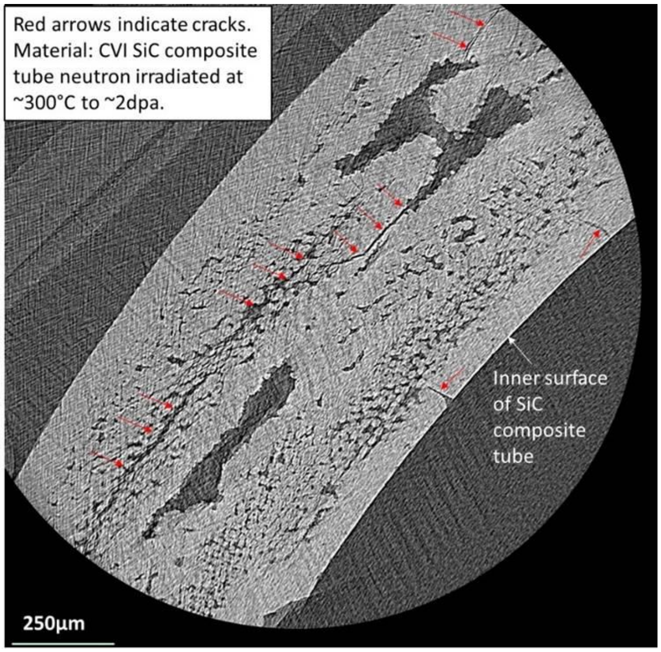

Figure 9. Microcracks of SiC Composite Tubes observed by x ray computed tomography (XCT) with a high-resolution setting.

- **[LANL]** Milestone M3FT-17LA020202042, "Oxide Morphology of FeCrAl following Extended Aging," was completed. The report documents results of an investigation of oxide formation at temperatures relevant to light water reactor cladding operation following extended aging to assess growth kinetics, chemical composition, and microstructure of oxide formation on a commercial FeCrAl alloy, Fe-21wt.%Cr-5wt.%Al-3wt.%Mo (Kanthal APMT). Coarsening of the native oxide layer is viewed as one potential means of mitigating tritium migration as may be important to deployment of FeCrAl alloys for BWR applications. Aging treatments were performed for 100-1000 hours in stagnant air at 300, 400, 500, and 600 °C, respectively. Oxide growth behavior under the investigated conditions follows a logarithmic time dependence. When the oxidization temperature is 400 °C or below, the oxide is amorphous. At 500 °C, isolated crystalline regions start to appear during short period aging time and expand with extended exposures. Crystalline α-Al_2O_3 oxide film develops at 600 °C and the correlated logarithmic rate constant decreases significantly, indicating enhanced oxidation resistance of the formed oxide film. In addition, Mo segregation at grain boundaries has been observed when the aging temperature exceeds 500 °C. The results of this study can be viewed as an upper bounding result for potential oxide coarsening during reactor operation. This work has been submitted to *Corrosion Science* where it is currently under review. FY18 work will extend these studies to optimized FeCrAl alloy compositions. (N. Li). (A. Nelson)

LWR Irradiation Testing & PIE Techniques

- **[INL]** Chemical analysis was performed on 3 samples from ATF-1A (SPS UO_2+ additives). The measured burn determined from these analyses were lower than the expected burnup from simulation. The cause of this discrepancy is being investigated. (J. Harp)

Rodlet	Measured Burnup (GWd/mtU)	Simulated Burnup (GWd/mtU)
ATF-1A R1	7.2	8.4
ATF-1A R4	4.9	6.31
ATF-1A R5	7.2	9

- **[INL]** All baseline PIE was completed on these first 3 rodlets from ATF-1. This satisfied a level 3 milestone on schedule. The results of these exams will be reported next fiscal year. (J. Harp)
- **[INL]** Dimensional exams were performed on ATF-1 FCA L3 (ORNL LOCA). No changes in dimensions were observed. A more thorough than usual exam was performed to attempt to detect any flaw that may be related to the previously observed fission gas release. (J. Harp)
- **[INL]** The Level 2 Milestone M2FT-17IN020203013 to finish the annual ATF-1 Irradiation status report was completed ahead of schedule on 9/27/17. (G. Core)
- **[INL]** All as-run data for ATF-1 experiments were compiled into a single document to support a single-source for modelling and experiment information. (G. Core)
- **[INL]** The Accident Tolerant Fuels 2 (ATF-2) Sensor Qualification Test (SQT) experiment was installed in the Advanced Test Reactor (ATR) 2A Loop on September 13, 2017 and System Operability testing was completed on September 27, 2017. ATR is scheduled for reactor startup on October 2, 2017 for cycle 162A. Fabrication of "low risk" ATF-2 (Fuel Test) components is in progress. ATF-2 fuel pin components are being machined and weld development is in progress. (G. Hoggard)
- **[ORNL]** A L3 milestone titled, "Irradiation of Wrought FeCrAl Tubes in the High Flux Isotope Reactor (HFIR)," has been completed. A report was issued summarizing the initiation of a series of irradiation experiments containing various engineering-grade FeCrAl alloy tube specimens beginning in HFIR cycle 472 (May 2017). These cladding tubes have representative 17 × 17 array pressurized water reactor fuel cladding dimensions and microstructure. The tubes will be irradiated at relevant temperatures (~340°C) and evaluated post-irradiation to determine irradiation effects on microstructure and mechanical properties for dose levels ranging from ~2 dpa to >20 dpa. (C. Petrie, K. Field, K. Terrani)
- **[ORNL]** A report titled, "Report on preliminary examination of deformation modes in Gen II FeCrAl alloys," was submitted to complete a Level 3 milestone (M3FT-17OR020203032). The report titled, "Deformation Behavior in a Neutron Irradiated Generation II FeCrAl Alloy for Accident Tolerant Fuel Cladding," provides the preliminary analysis of the deformation modes/mechanics in neutron irradiated ORNL-developed Generation II FeCrAl alloys. Complementary characterization to complete this analysis was performed using the neutron scattering and electron microscopy facilities housed at ORNL. Characterization efforts show similar irradiated microstructures compared to Generation I alloys irradiated under similar conditions. Preliminary studies show the ductile fracture of the Generation II FeCrAl alloy, C35M, can be linked to the formation of dislocation cells/tangles. This report provides critical insights into the deformation behavior of Generation II FeCrAl alloys. K. Field)
- **[INL]** The Level 2 milestone was met with the final release of the Metals Fuels Handbook: Parts 1 and 2. (C. Papesch)

- **[INL]** The year end status report titled, "Characterization Report on Fuels for NEAMS Model Validation," was finalized and sent to management to complete the L3 milestone. This is revision 1 and includes further data on the U3Si2 fuel composition. (C. Papesch)
- **[INL]** The year end status report titled, "Status report on the Development of a Thermodynamic Database for Use with New Fuel Alloy Design," was finalized and sent to management to complete the L3 milestone. (C. Papesch)

LWR Transient Testing

- **[INL]** Progress continued on comment resolutions for comments that were provided as part of the design review of the Multi-SERTTA-CAL device. Nearly all of the comments on the neutronic analysis have been resolved, and all of the comments have been resolved on the thermal analysis. The thermal analysis has been submitted for approval. Comments still remain to be resolved regarding the structural analysis, and subsequent drawing changes need to be incorporated. (J. Schulthess)

ADVANCED REACTOR FUELS

AR Computational Analysis

- **[INL]** The L3 milestone, "Status Report on Transmutation Fuel Performance Modeling Demonstrating Results on a Relevant Example Problem," has been completed. (P. Medvedev)

AR Fuels Development

- **[ANL]** The Level 3 milestone report titled, "Assessment of AmBB Performance and Tradeoff of Advanced Fuel Concepts – FY2017," was completed and submitted. In this report, the AmBB performance with fissile addition (which has been proposed by CEA to achieve a flat temperature distribution) was evaluated using high fidelity tools. Additionally, the impacts of annular fuel on two reactor performance parameters, fuel cumulative damage factor (CDF) and irradiation damage (DPA) of grid plate, were assessed, and it was tentatively concluded that the annular fuel associated with the lower gas plenum has a promising potential for increasing fuel burnup and extension of reactor lifetime. (T. K. Kim)
- **[ANL]** In order to produce physics parameters for planned analysis of fuel performance and transient behaviors of annular fuel in a SFR, sensitivity analyses were conducted using the Advanced Burnup Reactor (ABR). The conventional "solid fuel" employed U-Pu-10Zr with 75% smeared density, sodium bond, and targets 100 MWd/kg based on 4-batch scheme. The "annular fuel" option also employed U-Pu-10Zr fuel, but the smeared density was reduced to 55%, and active fuel length was increased 100 cm from 80 cm to compensate the reduction of smeared density. The "annular fuel" adopted 8-batch scheme to increase burnup to 200 MWd/kg. Table 1 shows the impacts of fuel choices and associated design specifications on the reactor physics performance. The burner design required higher TRU content to increase the burnup by a factor of two, which increased reactivity swing, and reduced breeding ratio. The increased driver fuel column helped to mitigate these effects by reducing the power density, but was responsible for higher pressure drop and sodium void worth. Even though the burnup is increased significantly, most physics parameters are acceptable or could be controlled with appropriate design features. However, the peak fast fluence is far beyond the current design practice and thus, a detailed fuel performance analysis is required to ensure the fuel integrity. A lower gas plenum could be a potential solution to achieve such a high burnup. (T. K. Kim)

Table 1: Sensitivity analysis on the annular vs. solid metallic fuels

	Solid fuel	Impact from changes in				Annular fuel
		smeared density	*bond type*	*fuel length*	*burnup and batches*	
Reactor physics performance						
Reactivity swing, pcm/cycle	2,540	*40.9%*	*1.2%*	*-10.3%*	*23.0%*	3,994
Breeding Ratio	0.84	*-18.0%*	*-1.0%*	*10.5%*	*-9.0%*	0.69
Avg. TRU content, %	24.3%	*43.0%*	*1.0%*	*-12.3%*	*18.9%*	36.6%
Avg. Power Density, W/cm^3	288	*0.0%*	*0.0%*	*-20.0%*	*0.0%*	231
Max. Power Density, W/cm^3	390	*8.2%*	*-8.7%*	*-18.0%*	*-4.2%*	303
Peak Fast Fluence, $10^{23} n/cm^2$	4.4	*-25.7%*	*-0.3%*	*15.5%*	*96.3%*	7.5
Peak Pressure Drop, bars	2.1	*0.0%*	*0.0%*	*16.1%*	*0.0%*	2.4
Beta effective, pcm	335	*-5.2%*	*-0.2%*	*1.3%*	*-2.4%*	313
K_D, $	1.0	*-4.3%*	*-3.6%*	*15.8%*	*-21.1%*	0.8
Sodium void worth, $	4.1	*-32.9%*	*35.0%*	*45.9%*	*13.7%*	6.1

- **[INL]** A new stirrer design was completed to improve the efficiency of the NpO2 reduction process. (L. Squires)
- **[INL]** Acceptance testing of the stoichiometry control system has been completed. September testing focused on the control software and sintering furnace operation. During the testing phase several changes were made to the software to ensure the appropriate parameters were configured and recorded correctly. Furnace control was also tested to ensure the furnace operated as programmed. Previous to this testing, all furnace operations were performed by programming the furnace controller directly. Directly programming the furnace controller has been shown to be a complicated process in which errors can be easily made. In order to make furnace programming more intuitive, the system control software is now used to program the furnace controller, thereby lessening chances of an error being made. This control was tested and the furnace further tuned to improve the overall furnace control.
- After the final testing was accepted, MOX fabrication trials were initiated meeting a level 3 milestone to initiate MOX fabrication activities. Several $(U_{0.8}Pu_{0.2})\ O_2$ pellets were pressed and sintered. A cover gas of argon with 500 ppm moisture was used to control the sintering atmosphere. Figure 10 below shows a typical example of the pellets being made. A second test will be performed using dry argon as a cover test to determine the effects of the moisture on the overall stoichiometry. Based on these two experiments further tests will be designed to better understand stoichiometry behavior of this system and determine if additional modification are needed in order to increase the amount of moisture present. (R. Fielding)

Figure 10. Example pellet.

- **[INL]** Traditionally, transmutation fuel has been produced through casting, however, other fabrication methods may also have benefits. A possible method of fuel fabrication currently being investigated is extrusion. Although extrusion will be difficult to implement remotely, it carries the advantage of possibly being able to produce long annular fuel slugs, in much the same way as tubing is currently extruded in other metal industries. To investigate the extrusion of U-10Zr and U-6Zr alloys, two extrusion billets of that composition have been cast and co-extruded with a zirconium can. The zirconium can was used to produce an integral FCCI barrier. Figure 11 below shows the billet during the canning process. The billet was slid into the zirconium can, leaving only a minimal gap between the fuel and can, and a lid seal welded on using gas tungsten arc welding. After welding, the can was heated to 800°C in a salt bath and extruded using a 150 ton Butech-Bliss extrusion press. The final extruded rod was approximately 6 mm in diameter and a typical section is shown in Figure 12. After extrusion, the rod was visually examined and no evidence of failure was found. (R. Fielding)

Figure 11. U-10Zr and zirconium can just prior to assembly and seal welding.

Figure 12. Typical section of the co-extruded Zr/U-10Zr rod.

AR Core Materials

- **[LANL]** Final ring pull testing has been completed on the BOR-60 irradiated 14YWT tube. Data showed very low ductility resulting from microcracks which were present before irradiation. This data was added to the L2 milestone and submitted by the end of September. (T. Saleh)
- **[PNNL]** Hardness testing has been started on several neutron irradiated materials in support of the milestone M3FT-17PN020302042. Three alloys are currently being tested. (M. Toloczko)
- **[PNNL]** A draft report comparing the microstructure of 14WYT ion irradiated to high dose at KIPT and TAMU has been completed. The intent is to assess how strongly the use of different accelerators affects the outcome of high dose ion irradiation studies. The KIPT accelerator irradiated with Cr at a very high dose rate while the TAMU accelerator irradiates with Fe at a lower dose rate the KIPT. This study attempted to take advantage of independent experiments on 14YWT in the two accelerators.

While 14YWT was used for both studies, the fabrication processing steps were somewhat different for the two versions of 14YWT resulting in slightly different starting microstructure. Comparisons of the microstructure after irradiation are showing different trends in their response, and it is unclear whether this is due to the different accelerator operating conditions or the starting condition of the materials. This experiment will be repeated by irradiating the KIPT 14YWT at TAMU. (M. Toloczko)

- **[PNNL]** A manuscript on the topic of identification of carbon contamination in ion irradiated materials that was submitted to *Scientific Reports* has come back from review, and changes are being incorporated based on the minor review comments. This manuscript is expected to be published in late October or early November. (M. Toloczko)
- **[PNNL]** Hardness testing was completed on several neutron irradiated materials in support of the milestone M3FT-17PN020302042. (M. Toloczko)
- **[LANL]** Three 25 cm long tubes of 14YWT were hydrostatically hot extruded at CWRU. The tubes were 7 mm in diameter and have a 0.5 mm wall thickness. The material that was extruded was from CEA as part of the bilateral collaboration. Characterization of these tubes is underway. (S. Maloy)
- **[ORNL]** A report was submitted in successful completion of milestone MF3FT-17OR020302031 titled "Status Report Documenting Development of Friction Stir Welding for Joining Thin Wall Tubing of ODS Alloys," for the Advanced FR Cladding program with the Nuclear Technology Research & Development Advanced Fuel Campaign. This report summarizes the development of friction stir welding (FSW) as a method for welding a thin plate of the advanced ODS 14YWT ferritic alloy. The report covers the tensile properties and plastic deformation behavior of miniature tensile specimens that were fabricated from the base metal (BM) and stir zone (SZ) of a 1 mm thick plate of 14YWT containing the FSW weld. Digital image correlation (DIC) was used to characterize the miniature specimens during in-situ tensile testing. The important findings provided by this technique was that the SZ specimens showed only a slight decrease in strength, with no loss of ductility, compared to the BM specimens and that the strain localization behavior between SZ and BM specimens were similar. Based on these results, FSW shows great promise as a method for joining thin sections of advanced ODS alloys. This work is novel since no other studies have explored FSW for joining thin sections (1 mm or less) of advanced ODS alloys. (D. Hoelzer)
- **[ORNL]** The residual stress data obtained from experiments conducted on the HB-2B beam line at the Neutron Residual Stress Facility at HFIR were processed and analyzed. The neutron scattering experiments were performed on four plates of 14YWT (SM13 heat) that were rolled to different thicknesses and deformation magnitudes during fabrication of the 1 mm thick plate used in the friction stir welding (FSW) study. The results showed that residual strains accumulated in each plate with increasing rolling deformation magnitude. The dependence of the residual strains on orientation within the plates was obtained by scanning each plate in the extrusion (ED), rolling (RD) and normal (ND) directions. The results indicated that residual strains increased in ED and RD with increasing deformation magnitude but were insensitive to the deformation magnitude in ND. This observation was consistent with deformation occurring in plane in the plates during rolling. The estimate of residual stresses in the 1 mm thick plate showed a range in values from ~122 - 384 MPa, which is a substantial amount of stress that could influence the cracks that formed in the stir zone (SZ) of the 1 mm thick 14YWT plate. Additional residual stress measurements are planned in the next FY work package that will investigate the magnitude of residual stresses that are produced by FSW and the effects of post weld heat treatments on reducing the residual stresses to improve the FSW weld quality on thin sections of 14YWT. This research was awarded beam time on the ORNL Neutron Science User proposal (IPTS-18043.1) titled, "The Role of Deformation Magnitude during Hot Rolling of 14YWT Plates on Generation of Residual Stresses." (D. Hoelzer)

- **[PNNL]** Improvement of high temperature fracture toughness of HT9 steels has been pursued. Two series of thermomechanical treatments for original and nitrogen-doped HT9 steels were completed. Eighteen hot-rolled strips were produced for the two alloys, which were followed by normalization and quenching treatments. Non-traditional tempering treatments, the final step of processing, were applied to introduce fine microstructures. The first series of heat treatments were single-step tempering at 300–600°C and the second serious were two-step tempering (a 650°C tempering was added to the single-step tempering). Mechanical testing to screen processing conditions is planned. (T.S. Byun)
- **[PNNL]** As part of the program to fabricate tubing from difficult-to-fabricate materials, MA956 and 14YWT are being extruded and pilgered to final dimensions. An existing PNNL rolling mill has been modified so that pilgering can be conducted. An initial set of runs to check out the pilgering modifications has been completed and was successful. The initial checkout runs consisted of pilgering flat plates with three different materials. The materials were copper, stainless, and magnesium in that order. Programming modifications are being made to the electronics based on the results of these initial runs. Insofar as pilgering for tube shapes is concerned, the next activity is to design the tooling, particularly the mandrels and rollers. This will begin as soon as the expert resources currently devoted to the pilgering modifications to the rolling mill become available. (R. Omberg)

AR Irradiation Testing & PIE Techniques

- **[INL]** The L2 Milestone, "Complete Conceptual Design of Advanced Coatings/Liners Experiment (AFC-4F)," was completed on 9-28-2017. Conceptual design completion is the first step in the design process where the path to be taken for final design is clarified. (D. Dempsey)
- **[INL]** Chemical analysis was performed on AFC-4A. These analyses allow for the calculation of burnup and comparison to predicted burnup from simulation. There was very good agreement between the measured and simulated burnup in this experiment (Table 2). (J. Harp)

Table 2. Comparison of Measured vs. Simulated Burnup

Rodlet	Measured Burnup (%FIMA)	Simulated Burnup (%FIMA)
AFC-4A R1	2.59%	2.41%
AFC-4A R3	2.20%	2.51%
AFC-4A R4	2.69%	2.55%
AFC-4A R5	2.52%	2.51%

- **[INL]** All baseline PIE was completed on AFC-4A. This completed a level 3 milestone. The results of the exams on AFC-4A will be reported in FY 18. (J. Harp)
- **[INL]** A report titled, "Testing Fast Reactor Fuels in a Thermal Reactor: A Comparison Report," (INL/EXT-17-41677) was issued. This report documents a comparison between specific fuel compositions irradiated in a true fast spectrum in the Phenix reactor (FUTURIX-FTA) and a pseudo-fast spectrum irradiation in the Advanced Test Reactor (AFC series). This report demonstrates that testing in the Advanced Test Reactor creates conditions that are similar to what is produced in a true fast spectrum reactor, and fuel performance phenomena that are primarily dependent upon temperature and temperature gradient inside the fuel can be adequately tested in the Advanced Test Reactor. The release of this report satisfied a level 2 milestone. (J. Harp)

- **[ORNL]** A Level 3 Milestone (M3FT-17OR020303031) titled “Complete Irradiation of Parallelepiped Rabbits & Prepare for Shipment to INL,” for the Accident Tolerant Fuel (ATF) program within the Fuel Cycle Research & Development Advanced Fuel Campaign was successfully completed and reported in September. The technical report summarizes the work undertaken at Oak Ridge National Laboratory (ORNL) during FY17 in support of the Fuel Cycle Research and Development's Advanced Fuels Campaign's effort on low-dose irradiation testing of metallic fuels for advanced fast reactors. A campaign of irradiation testing of parallelepiped specimens in irradiation vehicles called rabbits has been completed, of which one rabbit capsule remains at ORNL as it cools following the irradiation -- successfully completing this portion of the work package. Furthermore, it was determined mid-way through the year that the rabbit capsules designed for TEM-disk shaped specimen irradiations were to be opened at ORNL facilities. This was also successfully completed with the internal components removed from the outer housings. However, it was noted that during the irradiation, some of the Gd-cups that housed the specimens in the TEM-disk campaign had fused/bonded together during the irradiation and more effort will be required to fully remove the material samples from these Gd-cups. (P.Edmondson, R.Howard, K.Linton)

CAPABILITY DEVELOPMENT

Irradiation, Testing, and PIE

- **[INL]** EXAFS measurements at the Advanced Photon Source were initiated, but not completed due to beam shut down. Data analysis and interpretation of the EXAFS experiments is continuing in unirradiated and irradiated uranium to examine bond length, coordination number, and disorder. A graduate student is learning X-ray diffraction (XRD) software, FIT-2D, to begin to interpret the XRD results from low fluence measurements at NSLS II. (M. Okuniewski)

For more information on Fuels contact Jon Carmack (208) 533-7255.

MATERIAL RECOVERY AND WASTE FORMS DEVELOPMENT

CAMPAIGN MANAGEMENT AND INTEGRATION

- **[PNNL]** All work packages have been input, reviewed, and approved by NTD and DOE (J. Vienna)

REFERENCE TECHNOLOGIES AND ALTERNATIVES

- **[ORNL]** In preparation for a planned kilogram-scale hot cell demonstration with used nuclear fuel (UNF), three runs of the iodine and tritium capture systems were completed successfully on September 18, 2017. All samples have been submitted for analysis. The analysis results and data analysis will be covered in a subsequent report to be issued by the Off-Gas Sigma Team. Further tests should be undertaken to provide additional information on the systems performance. The objectives are provided for the additional tests and test conditions. The associated milestone, M3FT-17OR030102032 “Cold testing of tritium and iodine traps prepared by off-gas sigma team,” was completed on schedule. (B. Jubin)
- **[ORNL]** The ORNL “Nuclear review panel” reviewed the plans for a hot demonstration for FY2018 and identified that the nuclear fuel powders generated by the process have no disposition path. Before the demonstration could proceed, an acceptable waste form and a disposition path need to be identified. A redirection of efforts during FY18 to focus on a research task providing a disposal waste form for the fuel powder would provide a path forward for future hot experiments and demonstration. (B. Jubin)
- **[ORNL]** A report was issued that completed milestone M3FT-17OR030107021, “Performance evaluations of cation exchanged SAPO membranes on alumina supports.” The report describes the synthesis and evaluation of molecular sieve zeolite membranes to separate and concentrate tritiated water (HTO) from dilute HTO-bearing aqueous streams. In the first phase of this effort, several monovalent and divalent cation-exchanged silico alumino phosphate (SAPO-34) molecular sieve zeolite membranes were synthesized on disk supports and characterized with gas and vapor permeation measurements. In the second phase, Linde Type A (LTA) zeolite membranes were synthesized in disk and tubular supports. The pervaporation process performance was evaluated for the separation and concentration of tritiated water.

  The report also describes the experiments that were performed using tritiated water feed solution containing tritium at the high end of the range (1 mCi/mL) anticipated in a nuclear fuel processing system that includes both acid and water streams recycling. The tritium concentration was about 0.1 ppm. The permeate was recovered under vacuum. For the ion exchanged SAPO-34 zeolite membrane, the HTO/H_2O selectivity and separation factor calculated from the measured tritium concentrations ranged from 0.99 to 1.23, and 0.83-0.98, respectively. Ion exchanged K-LTA membranes performed better with a separation factor ranging from 1.3 to 2.79. Due to the high water permeance, HTO is retained and concentrated on the feed side compared to SAPO membranes where HTO was slightly more concentrated in the permeate. Several encouraging observations including molecular sieving and high vapor permeance suggesting a path forward to further improve both permeance and separation factor are discussed. (R. Bhave, B. Jubin)
- **[ORNL]** In the month of September, the focus was on the techno-economic analysis of the zeolite membrane based tritiated water concentration. The analysis and comparison of the membrane-based tritium separation and concentration with the CECE system is nearly complete, and the draft of the milestone report will be submitted for reviews and approvals in the next few days. (R. Bhave, B. Jubin)

Sigma Team for Advanced Actinide Recycle

- **[INL]** An irradiation campaign was conducted to collect Am(VI) reduction data in the presence of excess zirconium. It was found that 5 mM Zr had no effect on the reduction rate of Am(VI) under gamma irradiation. This is an important finding since the reduction of Am(VI) in a radiation filed will occur in the presence of Zr as a constituent of the raffinate or dissolution. The investigation of other constituents is ongoing. This result, and those for Ce and U were summarized in NTRD-MRWFD-2017-000164 (B. Mincher)

Sigma Team for Off-Gas Capture and Immobilization

- **[INL]** A first iodine adsorption testing using 1-iodobutane, as a surrogate for organic iodides, was completed. This test used silver Aerogel for the sorbent and was designed to emulate dissolver off-gas conditions. The cumulative operating time for this test exceeded 400 hours. Initial results of this test are consistent with results in prior years of organic iodide adsorption testing using methyl iodide:

    1. Only a small percentage, if any, of the premixed iodobutane reacted with the NOx (nominally around 10,000 ppm by volume) and moisture (at 0.59 vol%, corresponding to a dewpoint of around in the simulated gas mixture upstream of the sorbent beds,
    2. Iodine adsorption followed the expected mass transfer zone theory of nearly quantitative adsorption at the front of the bed, with gradual adsorbed buildup of iodine in the front of the bed as the front of the bed gradually approaches saturation and the active adsorption zone (the mass transfer zone, MTZ) progresses through the depth of the bed,
    3. Apparent breakup (destruction) of the iodobutane molecule, as the sorbent adsorbs the iodine,
    4. Iodine capture efficiencies (decontamination factor, DF) exceeding 1,000-3,000 (based on measured detection limit values), until the sorbent approaches saturation, when the iodine decontamination factor approaches 1 (0% capture efficiency). Higher DFs might have occurred, but could not be detected.
    5. Continued nearly quantitative breakup of the iodobutane molecule, even after the sorbent approaches saturation; but the iodine that was not adsorbed remained in the gas stream, in the form of iodine species soluble in 0.3 N NaOH solution (such as I2 and HI).
    6. The sorbent in beds 1 and 2 (0.5 in. and 1.5 in. deep, respectively, for a total of 2 in.) approached saturation. The sorbent in beds 3 and 4 (2 in. and 4 in. deep, respectively, for a total bed 1-4 depth of 8 in.) did not approach saturation as much. (N. Soelberg, Welty)

- **[INL]** A level 3 Milestone M3FT-17IN030107012, "Optimize desorption techniques to evaluate gas product compositions," was completed and the results documented in a report titled “Preliminary Desorption Studies for HZ-PAN and AgZ-PAN”, NTRD-MRWFD-2017-000207. These studies were intended to be preliminary in nature, providing sufficient data to direct further research for desorption optimization of AgZ-PAN and HZ-PAN. Results indicate that further separation of Kr and Xe from the bulk gas stream should be possible with careful control of pressure and/or temperature during desorption. For HZ-PAN, the bulk of the Kr was removed with vacuum, minimizing sweep gas volume necessary for desorption. This is of particular interest as it may help to minimize volume of the final Kr waste form.

    Although the effluent streams from desorption have not yet been fully characterized, there is sufficient information from GC-TCD analysis to suggest that components present in air are adsorbed to some extent on both sorbents. Further research is necessary to determine the concentration of air and other undesirable species on the sorbent and if the gaps identified during this research may be exploited to achieve further separation of Kr and Xe from each other and the bulk gas stream. (Garn/Greenhalgh/Welty)

- **[ORNL]** To conserve funds for FY18, the activity to determine the impact of variations in NO, NO_2 and water concentrations on iodine adsorption rates has received lower priority. The associated milestone, M3FT-17OR0301070217, due 3/31/17 will be completed by 4/30/18. There will be no impact to the M2 milestone. (S. Bruffey, B. Jubin)
- **[ORNL]** Issues with ensuring a known, stable flow of CH_3I were identified during completion of the Level 2 VOG effort, which also used the CH_3I feed streams. An alternate means to supply the CH_3I was identified and a quote was received for the unit. This will be procured in October with a 12 week delivery time. Also to conserve funds for FY18, this activity will receive lower priority. The associated milestone, M3FT-17OR0301070218, will be completed by 5/30/18. There will be no impact to the M2 milestone. (S. Bruffey, B. Jubin)
- **[ONRL]** A total of 27 samples were prepared and have been HIPed for the Hot Isostatic Pressing of Engineered forms of I-AgZ task. Density measurements have been completed on each of these samples. X-ray diffraction analysis has been performed on 19 of these samples, with 8 outstanding. All samples exhibited the same six phases present: (1) Triclinic SiO_2, (2) FCC Silver, (3) FCC FeNi alloy (from the HIP casing), (4) AgI (Iodargyrite), (5) $Mg_2Al_4Si_5O_{18}$ (Indialite), and (6) Mordenite (token composition: $K_{1.5}NaCaAl_{4.5}Si_{19.5}O_{48}(H_2O)_{14.5}$). All samples will be examined by optical microscopy, which will complete the analyses planned for these samples. The time required to prepare the samples, section each one and complete the XRD was longer than expected and the completion of the initial analysis phase of these samples is now planned for October 30, 2017. (S. Bruffey, B. Jubin)
- **[ORNL]** Three experimental tests have been completed for the performance of Ru removal systems in prototypical TOG streams task. The first test determined the release rate of Ru in the test system. Ru was oxidized by O_2 at 700°C for 5 hours. The total amount of Ru recovered in the effluent stream (i.e. not lost to system components was less than 1 mg. Ru was found to be released at a variable rate over the course of the test. The second test exposed a metal mesh sorbent (held at 150°C) to a Ru-bearing gas stream. No Ru was observed in the effluent stream. The third test exposed a silica sorbent (held at 40°C) to the Ru-bearing gas stream. Breakthrough was observed, with Ru present in the effluent stream at hour 3 of testing. The silica gel will be analyzed to determine Ru content, but visual examination of the sorbent indicates uneven distribution of Ru through the sorbent bed. Experimental work is continuing with at least 3 more runs planned for early October. The expected completion date is November 30, 2017. (S. Bruffey, B. Jubin)
- **[ORNL]** A report was issued on September 29, 2017 describing the “Preparation of Hot Isostatically Pressed AgZ Waste Form Samples.” This completes milestone M3FT-17OR0301070211 on schedule. The base mineral contained in the samples include AgZ (in pure and engineered forms), silver-exchanged faujasite, and silver-exchanged zeolite A. Two iodine loading methods, occlusion and chemisorption, have been explored. Additionally, the effects of variations in temperature and pressing of the process have been examined, with temperature ranges of 525-1100°C and pressure ranges of 100-300 MPa. All of these samples are available to collaborators upon request. The sample preparation detailed in this document is an extension of that work. In addition to previously prepared samples, this report documents the preparation of additional samples to support stability testing. These samples include chemisorbed I-AgZ and pure AgI. Following sample preparation, each sample was HIPed by American Isostatic Presses, Inc. and returned to ORNL for storage until requested by collaborators for durability testing. The sample set reported here will support waste form durability testing across the national laboratories and will provide insight into the effects of varied iodine content on iodine retention by the produced waste form and on potential improvements in waste form durability provided by the zeolite matrix. (S. Bruffey, B. Jubin)
- **[ORNL]** A total of five runs have now been completed to examine the effectiveness of silica gel and 3A MS as tritium sorbents and silver-nitrate-impregnated alumina as an iodine sorbent for application

in the off-gas treatment for an advanced tritium pretreatment system. The runs are listed in Table 1 below. The first three of these were the tests associated with the milestone M3FT-17OR030102032, “Cold testing of tritium and iodine traps prepared by off-gas sigma team,” reported as part of the Volatilization Methods Work Package. Tests 4 and 5 selected from the recommended additional tests in that milestone report and focused on obtaining additional baseline data. The testing was performed according to the procedure listed in the milestone report except for Run 5, which contained no sorbent and did not pass flow through the sorbent columns and as a result the column desorption steps were omitted. Results are expected in mid-October and completion of the milestone M3FT-17OR030107026 by the end of October. (S. Bruffey, B. Jubin)

Table 1: Tests completed to assess performance of iodine and tritium removal system.

Run Number	Tritium sorbent	Alumina present	Iodine present
Run 1	None	Yes	No
Run 2	Silica gel	Yes	Yes
Run 3	3A MS	Yes	Yes
Run 4	None	Yes	No
Run 5	None	No	No

WASTE FORM DEVELOPMENT AND PERFORMANCE

Electrochemical Waste Forms

- **[ANL]** Electrochemical tests with RAW-6(UTc) are in progress to measure model parameter values. Figure 13a shows the microstructure and Figure 13b shows the potentiodynamic scans in pH 3b and pH 8b brine solutions. Phase 1 is an Fe-Cr-Mo intermetallic phase that hosts Tc and Phases 2z and 2u are an Fe-Zr-Ni intermetallic that hosts U, in which the brighter 2u regions have higher U contents than the 2z regions. Both Ru and Pd are enriched in the 2u regions. Figure 13c shows an EDS line scan performed through Phase 2 (see arrow in Figure 13a) showing the variance in the relative Zr and U concentrations. The PD scans show all phases are passivated and corrosion resistant to voltages that are well above the Eh values likely to occur in disposal systems. The addition of small amounts of trim Cr, Ni, and Mo to RAW-6(UTc) greatly improved the corrosion resistance of all constituent phases, including those hosting key radionuclides. The transpassive behaviors seen at about 0.8 V in the 3b solution and at about 1.0 V in the 8b solution are attributed to corrosion of the 2u and 2z regions of Phase 2. The corrosion resistance of Phase 2 benefits from the presence of Ru and Pd due to the electrochemical effects of the noble metals (i.e., generation of H_2). Potentiostatic tests are in progress to measure the steady-state corrosion rates of RAW-6(UTc) at several potentials in several solutions. (W. Ebert).

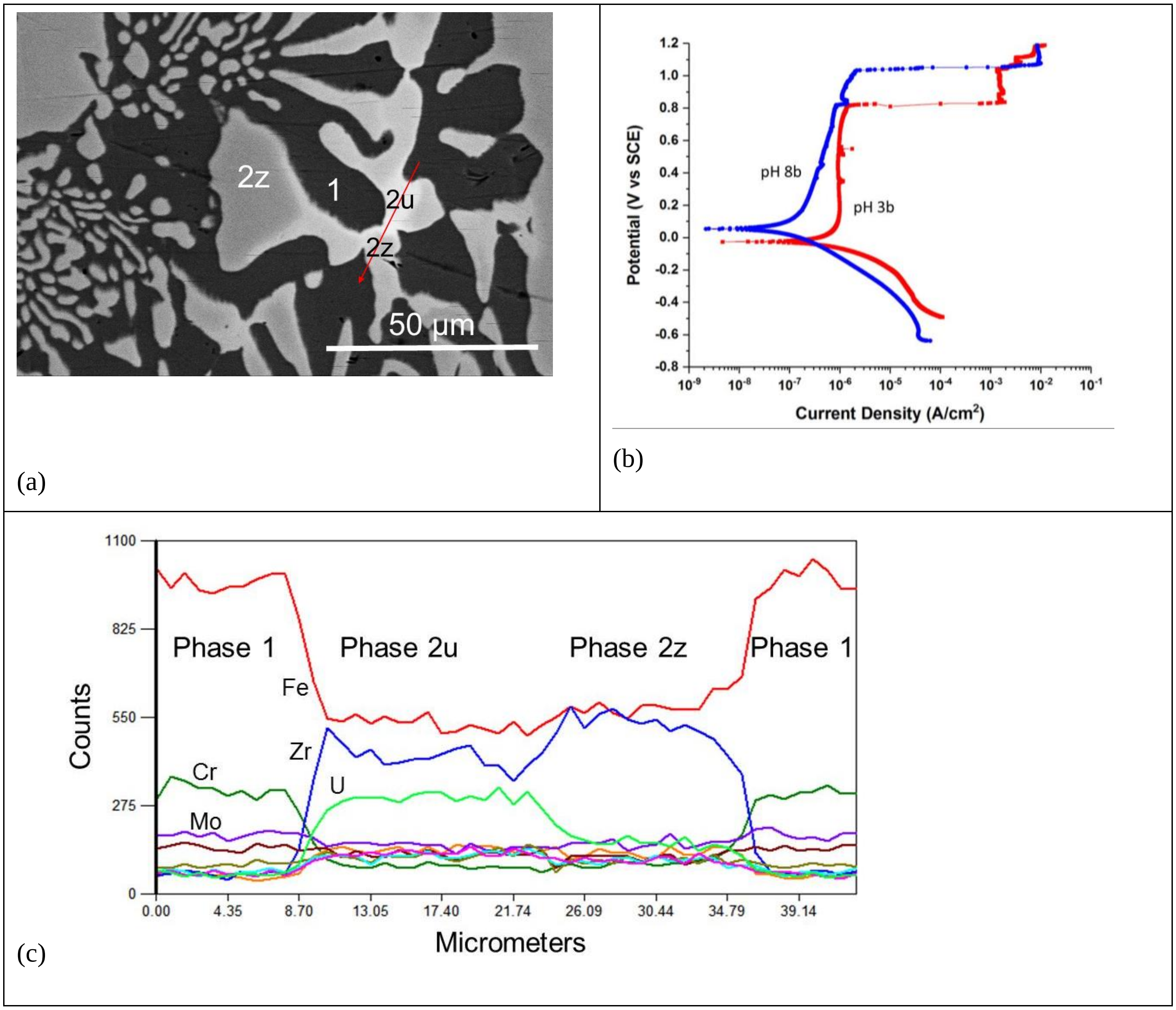

Figure 13. (a) Microstructure of RAW-6 (UTc), (b) potentiodynamic scans in pH 3 and pH 8 brine solutions, and (c) EDS lines scan through Phase 2.

- **[ANL]** The electrochemical method developed to evaluate metallic waste forms is being applied to Type 4320 carbon steel to demonstrate the applicability of the method and model to engineering metals that do not passivate, and Figure 14 shows resent results of electrochemical tests. Figure 14a shows the steady-state corrosion currents measured at several fixed voltages near the open circuit corrosion potential Ecorr. The current decreases initially due to a passivation layer formed in air over the time between when the surface was polished and immersed. The surfaces stabilize further due to transient passivation in solution and cathodic currents were measured for short durations in tests at the lower imposed voltages. However, the Cr and Mo that provide the initial passivation are leached and passivation is not sustained. The currents increase slowly to steady-state values representing the Cr- and Mo-depleted surfaces. The higher currents measured at higher applied voltages represent the sensitivity of the corrosion rate to the solution redox. Figure 14b shows the steady-state rates (data points) to be higher than the currents measured in a potentiodynamic scan of a polished surface (curve). Figure 14c shows Tafel scans before and after the potentiostatic test at -0.585 V_{SCE}, which is the Ecorr value determined for the fresh surface, which show the surface is destabilized during corrosion. The Tafel scans show Ecorr decreases and Icorr increases. The features in the anodic legs of the scan near -0.5 V_{SCE} (indicated by the arrow) are effects of the multi-phase surface, which are more evident before than after the hold. Figure 14d is an SEM image of the corroded surface showing the pearlite and ferrite phases that comprise the 4320 steel and that the ferrite matrix corroded preferentially relative to pearlite inclusion phases. Furthermore, the ferrite within the eutectic structure of the pearlite is probably dissolved in preference to the matrix ferrite. Pearlite is a eutectic mixture of ferrite and C-rich cementite, which is seen in Figure 14d to be more corrosion resistant than ferrite. (W. Ebert).

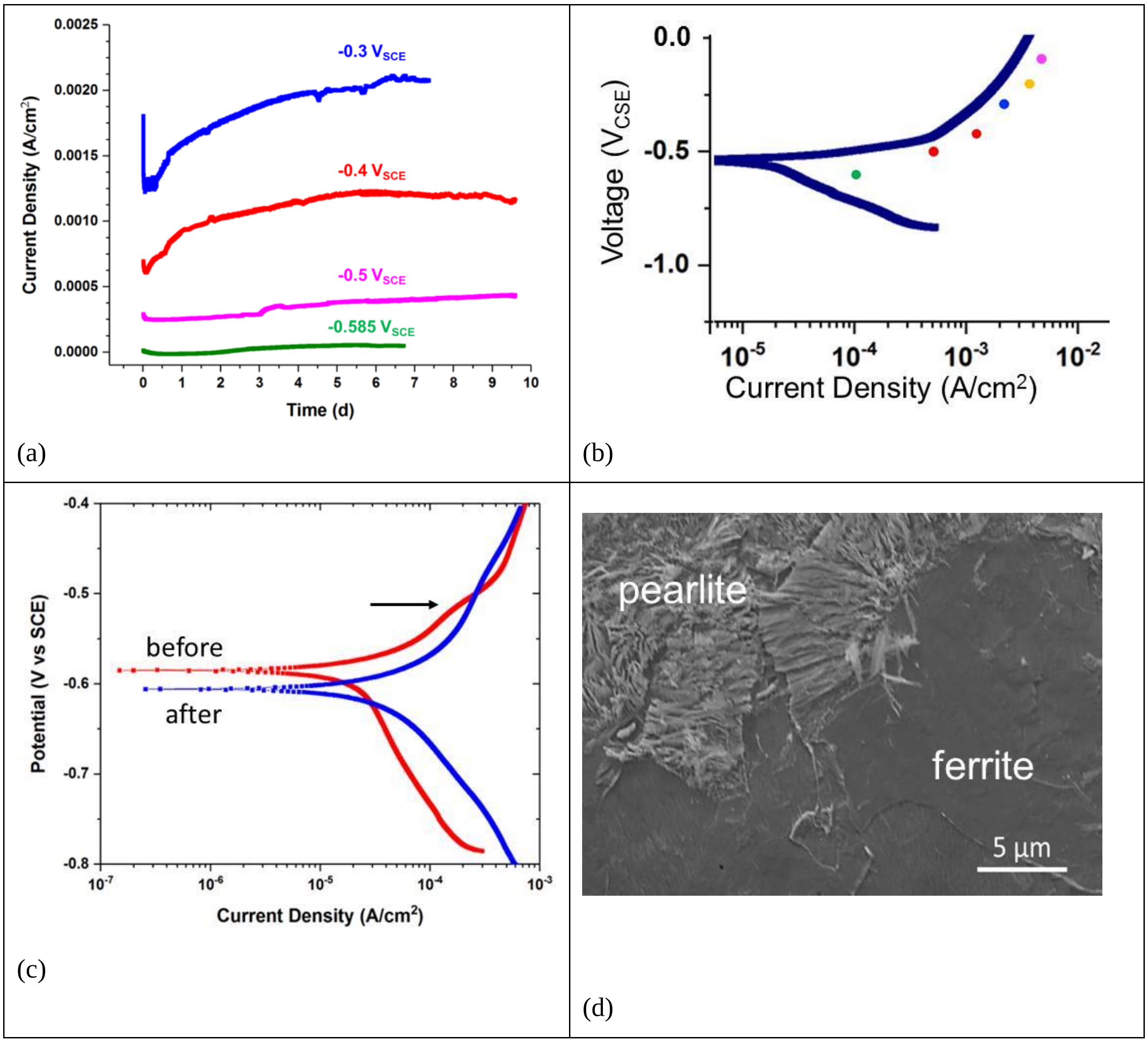

Figure 14. Results of potentiostatic test with Type 4320 carbon steel in pH 4 brine solution: (a) corrosion current at various hold voltages, (b) comparison with PD scan, (c) Tafel scans before and after potentiostatic test at -0.585 V_{SCE}, and (d) corroded surface after 7-day hold at -0.585 V_{SCE}.

The electrochemical tests for Type 4320 carbon steel are being compared with immersion tests with the same material conducted in the same solution at room temperature. Batch tests were conducted for various durations and the total mass loss (after wiping off the corrosion products and drying the specimen) was used to track the extent of corrosion. Figure *15*a shows the mass losses measured in tests conducted for up to eight weeks (data points) and Figure *15*b shows the corroded surface from the test conducted for two weeks. The linear mass loss seen for immersion tests conducted for increasing durations is consistent with the constant rates measured in the electrochemical tests at fixed potentials and the surface microstructures of the corroded specimens indicate the mechanisms are the same in the electrochemical and immersion tests. The average rate for the immersion tests was 9×10^{-5} g cm^{-2} d^{-1}, as shown by the solid line, whereas the electrochemical corrosion rate for the specimen held at -0.585 V_{SCE} was 5×10^{-4} g cm^{-2} d^{-1}, as shown by the dashed line in Figure *15*a. The lower rate measured in the immersion tests is attributed to the corrosion potential drifting to lower values throughout each test. This is consistent with the Tafel scans before and after the PS holds that indicate the corrosion potential decreases as the steel corrodes and is attributed to leaching of Mo and Cr from the surface during corrosion. This comparison provides further confidence for using the electrochemical testing approach and the model it supports to represent the long-term behavior of steel-based waste forms. (W. Ebert).

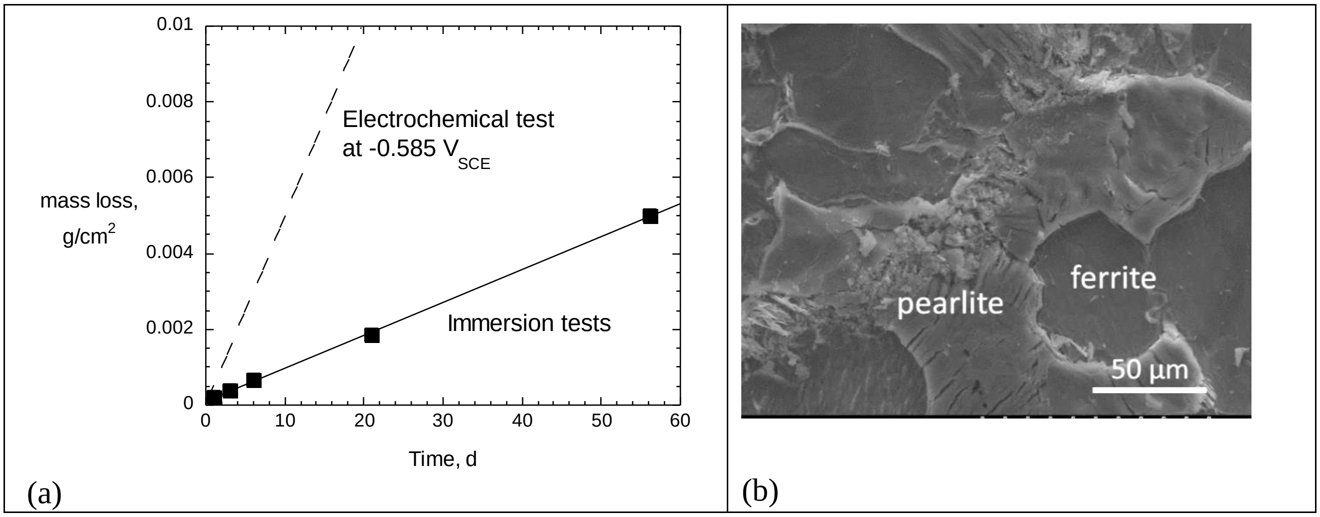

Figure 15. Results of immersion test with Type 4320 carbon steel in pH 4 brine solution: (a) mass loss and (b) corroded surface after 14 days.

- **[ANL]** A series of ASTM C1308 tests was completed with advanced SAP materials provided by KAERI. Solution analyses have been completed and are being evaluated. The atomic force microscope (AFM) has been repaired and analyses of SAP materials reacted in phosphate solution to attenuate the dissolution of phosphate phases are being completed for comparison to similar tests conducted in demineralized water. These will provide solids analyses to combine with solution analyses showing the effects of silicate and phosphate solution to support a mechanistic model for SAP waste form corrosion. (W. Ebert)
- **[ANL]** Solution analyses have been completed for ASTM C1308 tests conducted with an initial prototype iron phosphate glass waste form made with dechlorinated simulated waste salt from the electrorefiner. These tests provide insights used to develop test plans for work in FY 2018 to develop a dechlorination method and waste form. (W. Ebert)

Ceramic Waste Forms

- **[LANL]** Microcracks are observed in some He (alpha) ion beam irradiated multiphase ceramic waste form samples (from ANSTO and SRNL). The existence of microcracks could affect chemical durability of nuclear waste forms in long term storage. Although it has been reported in neutron irradiated and actinide doped ceramic waste forms before, to our knowledge, this is first observation of microcracks induced by ion beam irradiation in nuclear waste form. The SEM images in Figure 16 and Figure 17 below show microcracks in hollandite phase in both HIPed multiphase ceramic SW-1727 from ANSTO and melt-processed sample CAF-11113 from SRNL after 200 keV He irradiation at room temperature. In both pristine/unirradiated samples, no cracks are observed. It suggests that microcracks are induced by He irradiation damage. Another interesting observation is that cracks only occurred in hollandite phase, not in other crystalline phases. SEM images also tell us that the size of cracks in melt-processed ceramics is larger than that in HIPed samples. A further study is in progress to help us understand the formation of microcracks (M. Tang)

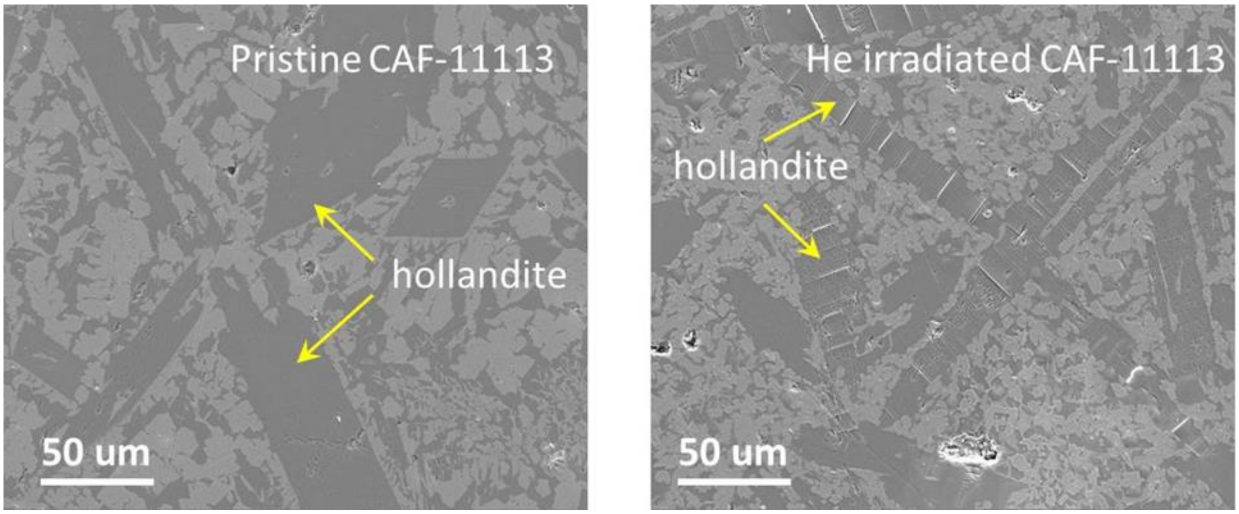

Figure 16. SEM images of pristine CAF-11113 (left) and He irradiated CAF-11113 (right).

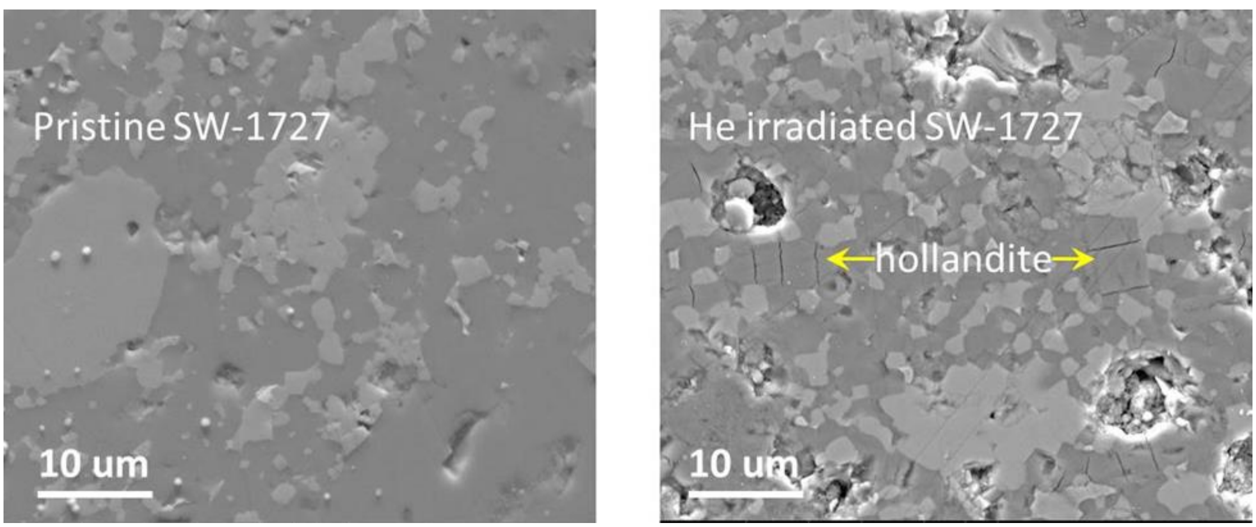

Figure 17. SEM images of pristine SW-1727 (left) and He irradiated SW-1727 (right).

Glass Ceramics Waste Forms

- **[LANL]** Microcracks are also observed in some He (alpha) ion beam irradiated multiphase glass ceramic waste form samples, single phase oxyapatite and powellite, and the remainder glass (based on the centroid composition named C1 with the crystals removed after slow cooling). The SEM images in Figure 18 show microcracks in He irradiated remainder glass but not in pristine glass. It suggests that microcracks are induced by He irradiation damage. Detailed results will be summarized in a future report. (M. Tang)

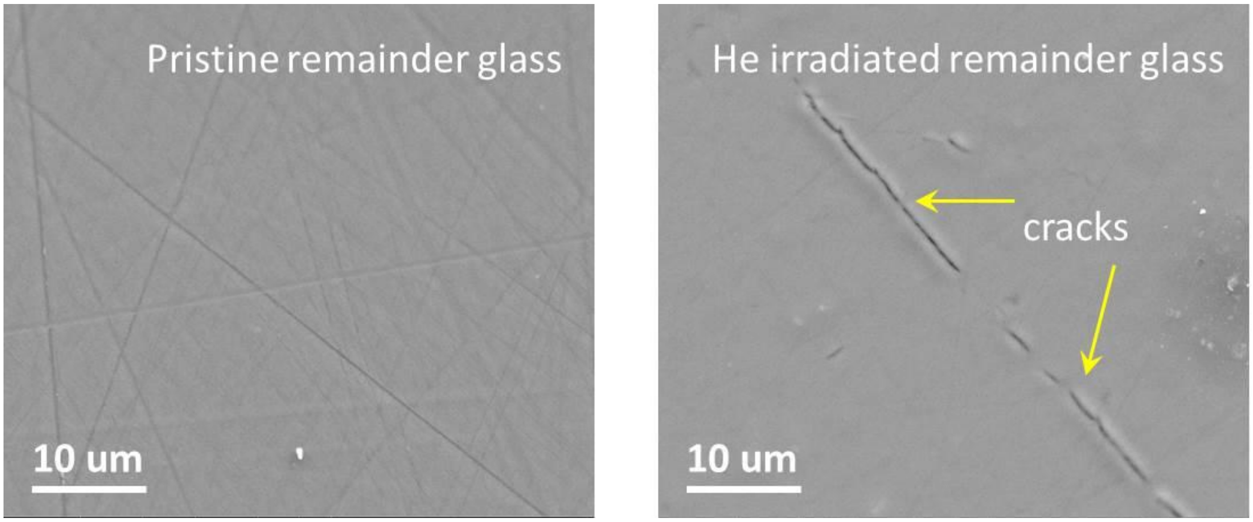

Figure 18. SEM images of pristine remainder glass (left) and He irradiated remainder glass (right).

Zirconium Recycle

- **[ORNL]** Extensive investigations of the source of the chlorination reactor pressurization problem, along with various modifications made to fix the problem, dominated activities during September. The cladding, boat, and filter/absorber unit were removed, and both the gas feed line and the $ZrCl_4$ vapor transfer tube between the reactor and condenser were cleaned mechanically but both of these tubes did not appear to be the source of plugging. Subsequently, the top of the condenser was removed and the condenser walls were observed to be essentially clean. However, upon disassembly of the filter/absorber unit, the zeolite absorber was found to be coated with a deposit of black solids which had a net weight of 6 g. The zeolite and black solids were transferred to a bottle and will be subsequently analyzed. Both the 40 um porosity inlet filter and the 10 um porosity outlet filter appeared to be clogged, presumably with the black substance. A new filter/absorber is being procured. Until it is available, we removed the inlet filter, bored holes in the outlet filter and filled the unit with glass wool to prevent entrainment during the chlorination unit when it is resumed. However, the plugging problem continued. After close inspection, we found that the feed line was partially blocked only when the reactor door was closed, due to a close tolerance into the ceramic block between the door and the boat. Thus, an additional half-inch was cut off of the gas feed line. All of these modifications were still not totally successful in removing the pressurization; therefore, we will investigate complete removal of the filter/absorber unit in early October. Due to these difficulties, the level 3 milestone will be delayed. (E. Collins, B. Jubin)

Advanced Waste Form Characterization

- **[ANL]** Long-term dissolution tests with AFCI and LRM surrogate glass waste forms are in progress. The available results are being used to derive the dependence of the residual and Stage 3 rates on temperature and the solution composition and determine solution conditions triggering the Stage 3 rate. Two tests have been terminated and the reacted solids are being analyzed to identify secondary phases that formed and the clay layers formed on the glass grains. The sampling intervals of the remaining tests have been increased to allow for longer overall test durations with sufficient solution. (W. Ebert).

- **[ANL]** Electrochemical tests with AgI fabricated as an electrode were completed in alkaline solutions at several applied potentials to extend the range of the data base generated to support future tests in which the solutions will be used to control the surface potential. The system to be used for tests with solution-controlled redox is being designed and tested. Our intent is to use an air-tight sealed system to avoid complications associated with a controlled-atmosphere glove box. (W. Ebert).

- **[PNNL]**A study of the TST rate model parameters based on glass composition has continued from earlier in the year. Recent efforts have focused on comparing the parameter values of high-level waste glass compositions and low-activity waste glass compositions. While there exists some variability in the rate model parameters for the glasses, two findings are particularly notable.

  First, the values for the parameters are rather close regardless of composition. This is not altogether an unexpected finding, as they are all based on the same aluminoborosilicate glass network. The exact impact of various components on the parameter values has not yet been determined, but they appear to be small. It is possible that all glasses in this family could be represented by the same set of parameters in the future, given a sufficiently large conservatism.

  Second, the parameters are highly correlated (Figure 19). The parameter sets themselves and the uncertainty ranges for each glass all fall on the same plane of correlated parameters. This means that if any two parameters of ko (initial rate constant), Ea (activation energy), and eta (pH influence) are known, then the third can be calculated. Additional research is being done to simplify the rate model to take account of these correlations. (J. Ryan)

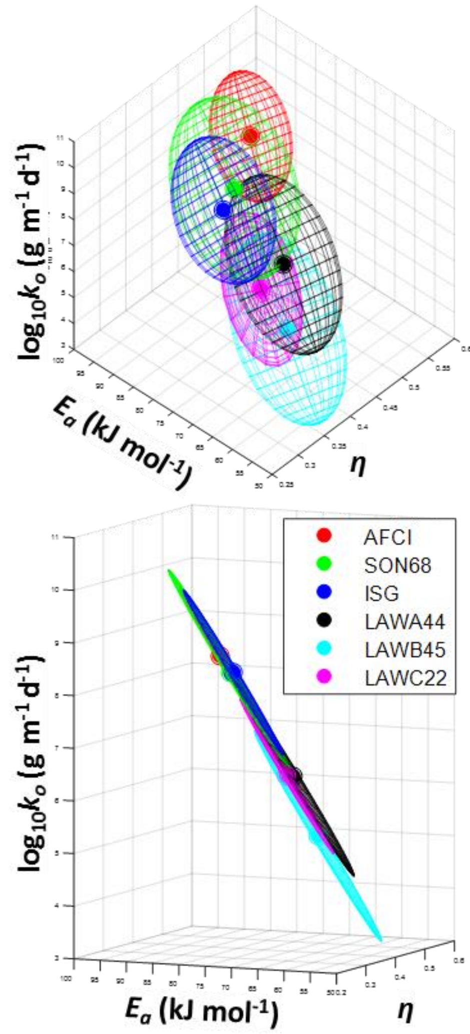

Figure 19. Two views of the principle component analysis of HLW (AFCI, SON68, ISG) glasses and LAW (LAWA44, LAWB45, LAWC22) glasses showing the common correlation between parameters for all compositions.

- **[PNNL]** Modeling/Simulation Fits with the GRAAL model to experimental data on aqueous concentrations of dissolved glass components from static corrosion tests often yield overestimated residual rates (left panel of Figure 20). This is because the model formulation, and in particular the equation that defines the time evolution of the gel layer thickness, was designed to reduce to a square root dependence on time at long times, whereas many experimental data sets exhibit gentler slopes. Therefore, we generalized the equation that controls the gel layer thickness by raising the unitless diffusion term by a power factor *p*, which significantly improved the quality of the fits (right panel of Figure 20). The modified model, GRAALP, was used to fit the long-term alteration data for a series of sodium borosilicate glasses reported by Gin *et al.* (JNCS 358 (2012) 2559) where glass alteration has slowed to a residual rate and growth of the gel layer has dominated alteration. The optimal value for the parameter *p* was found to vary significantly and could be correlated with glass composition. For the glasses containing both Ca and Al, a value of p = 3.0 was found most suitable and was reduced slightly to p = 2.6 if Ce was present in the glass. For glasses without Ca, the data followed the original GRAAL model with $p = 1.0$. In the absence of Al, glasses containing Ca and/or Zr were not as easily characterized. These findings point to a correlation between the residual alteration rate and glass composition. A power law dependence of diffusivity on local water content is proposed as a physical basis for these results. A detailed description and discussion of the improved model and its application can be found in milestone M3FT-17PN030105143 submitted this month. (S. Kerisit)

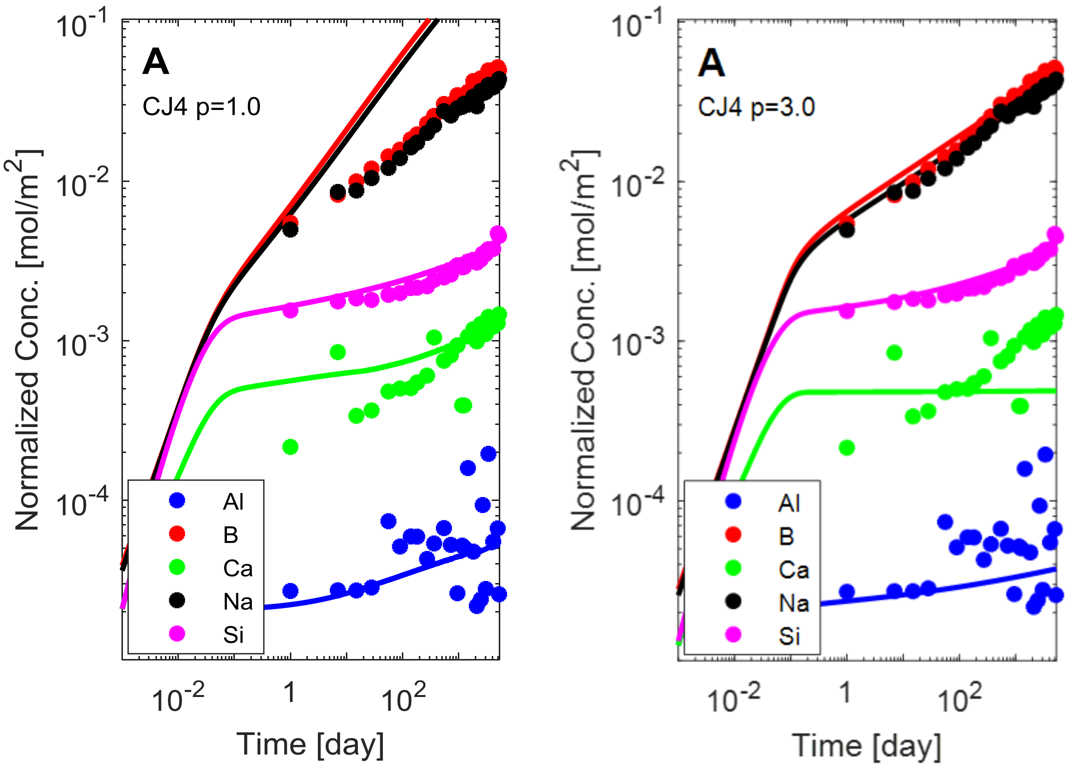

Figure 20. Fits to experimental data (Gin et al. JNCS 358 (2012) 2559) on aqueous concentrations of dissolved glass components from a static corrosion test of CJ4 (a.k.a. ISG) glass with original GRAAL model (left) and GRAAL model modified to include a power dependence (right).

FUEL RESOURCES

- **[ORNL]** A manuscript titled, “Origin of the Unusually Strong and Selective Binding of Vanadium by Polyamidoximes in Seawater,” has been accepted in *Nature Communications*: A. S. Ivanov, C. J. Leggett, B. F. Parker, Z. Zhang, J. Arnold, S. Dai, C. W. Abney, V. S. Bryantsev, and L. Rao. Origin of the Unusually Strong and Selective Binding of Vanadium by Polyamidoximes in Seawater. *Nature Comm.*, NCOMMS-17-16736B, 2017. **Abstract:** Amidoxime-functionalized polymeric adsorbents are the current state-of-the-art materials for harvesting uranium (U) from seawater. However, marine tests show that vanadium (V) is preferentially extracted over U and many other cations. Herein, we report a complementary and comprehensive investigation integrating ab initio simulations with thermochemical titrations and XAFS spectroscopy to understand the unusually strong and selective binding of V by polyamidoximes. While the open-chain amidoxime functionalities do not bind V, the cyclic imide-dioxime group of the adsorbent forms a peculiar non-oxido V^{5+} complex, exhibiting the highest stability constant value ever observed for the V^{5+} species. XAFS analysis of adsorbents following deployment in environmental seawater confirms V binding solely by the imide-dioximes.

Our fundamental findings offer not only guidance for future optimization of selectivity in amidoxime-based sorbent materials, but may also afford insight to understanding the extensive accumulation of V in some marine organisms. (V. Bryantsev and C. Abney)

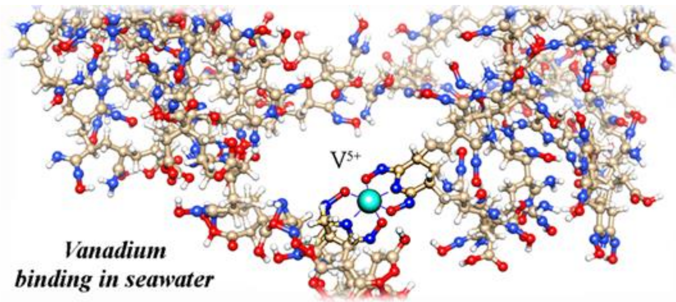

Figure 21. Vanadium binding in seawater

- **[ORNL]** A manuscript has been published in the journal, *Industrial & Engineering Chemistry Research* that relays the influence of hydrophilicity on brush-on-brush adsorbents. This technology was pursued to combine the benefits of the stable polyethylene trunks with the control of ATRP grafting. The results support the suggestion that hydrophilic trunks are preferred over less hydrophilic trunks. In addition to the published research, the manuscript is included in the inaugural 2017 Class of Influential Researchers, a program to recognize early career researchers. The manuscript can be found at the following link:

  http://pubs.acs.org/doi/10.1021/acs.iecr.7b00482?ref=VIarticle-iecred-researchers**.** (R. Mayes)

- **[ORNL]** A Level 4 milestone report, "Determination of Vanadium Binding Mode on Seawater-Deployed Polyamidoxime Adsorbents," was completed and submitted on Sept 29, 2017. Authors are Carter W. Abney, Vyacheslav Bryantsev, Alex Ivanov, Zhicheng Zheng (LBNL) and Linfeng Rao (LBNL). **Summary:** Adsorbents developed for the recovery of uranium from seawater display poor selectivity over other transition metals present in the ocean, with vanadium particularly problematic. To improve selectivity, an indispensable step is the positive identification of metal binding environments following actual seawater deployment. In this work, we apply x-ray absorption fine structure (XAFS) spectroscopy to directly investigate the vanadium binding environment on seawater-deployed polyamidoxime adsorbents. Comparison of the x-ray absorption near edge spectra (XANES) reveal marked similarities to a recently reported non-oxido vanadium (V) structure formed upon binding with cyclic imidedioxime, a byproduct of generating amidoxime functionalities. Density functional theory (DFT) calculations provided a series of putative vanadium binding environments for both vanadium (IV) and vanadium (V) oxidation states, and with both amidoxime and cyclic imidedioxime. Fits of the extended XAFS (EXAFS) data confirmed vanadium (V) is bound exclusively by the cyclic imidedioxime moiety in a 1:2 metal:ligand fashion, though a modest structural distortion is also observed compared to crystal structure data and computationally optimized geometries which is attributed to morphology effects from the polymer graft chain and the absence of crystal packing interactions. These results demonstrate that improved selectivity for uranium over vanadium can be achieved by suppressing the formation of cyclic imidedioxime during preparation of polyamidoxime adsorbents for seawater uranium recovery. (C. Abney)

- **[ORNL]** Two 5-gallon tanks with seawater from the Tampa Bay Desalination Plant in Florida, were used for batch experiments with AF1FR3 ORNL adsorbent. One of the tanks contained feed seawater into the desalination plant, while the other contained reject seawater. The goal of this experiment was to determine if the reject seawater from desalination plants is a better resource for uranium recovery than natural seawater. Analytical data received at the Marine Sciences Laboratory of PNNL have shown that, although the uranium concentration in the reject seawater of a desalination plant is twice the concentration in the feed seawater, the uranium adsorbed from reject seawater over 12 weeks was half the uranium adsorbed from feed seawater by the same adsorbent, over the same period of time. Specifically, 6.22 g U per Kg adsorbent were recovered from feed seawater of 2.9 ppb uranium concentration, and 3.95 g U per Kg adsorbent were recovered from reject seawater of 6.6 ppb uranium concentration. The reason of this unexpected behavior of the adsorbent is believed to be the higher concentration of iron, which competes with uranium, in reject water due to addition of iron as a coagulant in the pretreatment of seawater, prior to membrane desalination. Evidence of this hypothesis is the iron uptake over the 12-week period of the experiment. The adsorbent recovered 3.00 g Fe per Kg adsorbent from reject seawater, which went through pretreatment, and 1.06 g Fe per Kg adsorbent from feed seawater that was not pretreated. These results emphasize that the efficacy of uranium recovery from seawater by amidoxime adsorbents depends strongly on the type and concentration of other ions in seawater. (C. Tsouris)

- **[PNNL]** A manuscript titled, "Reusability of amidoxime-based polymeric adsorbents for seawater uranium extraction," has been accepted for publication in *Industrial and Engineering Chemistry Research.* The full citation for the Article First Web publication is:
  - Kuo, Li-Jung, Horng-Bin Pan, Chien M. Wai, Margaret F. Byers, Erich Schneider, Jonathan E. Strivens, Christopher J. Janke, Sadananda Das, Richard T. Mayes, Jordana R. Wood, Nicholas Schlafer, and Gary A. Gill (2017). Investigations into the Reusability of Amidoxime-Based Polymeric Adsorbents for Seawater Uranium Extraction. *Industrial and Engineering Chemistry Research,* Publication Date (Web): September 13, 2017, **DOI:** 10.1021/acs.iecr.7b02893. (G. Gill)
- **[Stanford]** Sea water selectivity tests are still ongoing based on a new type of sorbent material using electrochemical method. Performance optimization is still being investigated by exploring the parameter space. Also, long term sea water test based on new sorbent material is being investigated. (C. Liu)

CoDCon Demonstration

- **[ANL]** The analysis was completed and equations were updated describing U(IV) extraction behavior and redox chemistry to support flowsheet design for the CoDCon demo. The analysis was compiled into a report that was submitted to the NTD. The revised models and parameter values were applied to the U(IV) model equations included in the AMUSE code to improve simulation of U behavior in TBP-nitric acid systems. (C. Pereira)
- **[PNNL]** The following paper was accepted for publication in the peer-reviewed journal *Electroanalysis*:
  - A.M. Lines, S.R. Adami, A.J. Casella, S.I. Sinkov, G.J. Lumetta, and S.A. Bryan, Spectroelectrochemistry of the Pu (III/IV) and (IV/VI) couples in nitric acid systems. In this paper, the solution chemistry of Pu in nitric acid is explored via electrochemistry and spectroelectrochemistry. By utilizing and comparing these techniques, an improved understanding of Pu behavior and its dependence on nitric acid concentration was achieved. Here the Pu (III/IV) couple was characterized using cyclic voltammetry, square wave voltammetry, and a spectroelectrochemical Nernst step. Results indicated the formal reduction potential of the couple shifts negative with increasing acid concentration and reversible electrochemistry is no longer attainable above 6 mol/L nitric acid. Spectroelectrochemistry was also used to explore the irreversible oxidation of Pu(IV) to Pu(VI) and shine a light on the mechanism and acid dependence of the redox reaction. (G. Lumetta)

For more information on Material Recovery and Waste Forms Development contact Terry Todd (208) 526-3365

MPACT Campaign

MANAGEMENT AND INTEGRATION

Management and Integration

- **[INL]** Completed technical review of the MPACT Implementation Plan report to meet the L2 milestone and posted to PICSNE. Completed reviews of end of year status and milestone reports, and completed FY18 year milestone and budget planning. Presented a conference paper on pyroprocessing process monitoring technologies at the 2017 Global Conference in Seoul, South Korea.

SAFEGUARDS AND SECURITY BY DESIGN - ECHEM

Microfluidic Sampler

- **[ANL]** Installation of the flow cell version of the molten salt droplet generator in an inert atmosphere glovebox was completed. Initial testing of the system with molten salts showed that the valve system worked properly but other systems required further modifications before testing can be completed. A report entitled, "Fabrication and Testing of Generation 3 High-Temperature Flow Cell," that describes the design, testing, and glovebox installation of the of the microfluidic flow cell was completed and submitted to the NTD.

Modeling and Simulation for Analysis of Safeguards Performance

- **[ANL]** To support the MPACT Campaign virtual distributed test bed, the AMPYRE code has been modified to allow for flexibility in the timing and sequencing of unit operations in the electrochemical processing flowsheet. These changes enhance the ability of the model to simulate more realistic facility operation configurations and will support related studies involving the sequencing of operations, equipment sizing, and sensor interfacing. The AMPYRE parent function was restructured to handle the use of new MATLAB classes that represent unit operations and their input and output streams. Code defining the conversion of inputs to outputs has been extracted into functions for each unit operation, providing an enhanced system for evaluating alternative flowsheet options. A report entitled, "Unit Operation Sequencing for a Used Nuclear Fuel Electrochemical Processing Facility," that describes the changes made to the AMPYRE code to allow for flexibility in the timing and sequencing of unit operations.

Electrochemical Sensor

- **[INL]** End of year report was delivered.

Sensor for Measuring Density and Depth of Molten Salt

- **[INL]** End of year report was completed.

Voltammetry

- **[ANL]** Experimental activities were completed and a milestone report documenting the results of sensor development and performance evaluation was submitted to the program on 9/28/17. The work package for FY18 technology demonstration activities was developed and submitted.

- **[INL]** End of year report was completed.

Electrochemical Signatures Development

- **[LANL]** All FY17 work was concluded. The FY18 work package was submitted. Initial discussions with Brian Key and Eric Rauch regarding their FY18 work on Advanced Integration were held.

ADVANCED INTEGRATION

Advanced Integration (Methods)

- **[LANL]** A flowsheet with data is being developed, which will help to define "normal behavior". A diversion scenario will be chosen and work with the Microcalorimetry team will determine if integrating that sensor can indeed detect notional diversion. This exercise will answer questions such as, when, where, and how many sensors are needed for detection. These first steps will be repeated for other sensors and with Mike Fugate will help answer the "when, where, how many" questions through statistical analysis.

Advanced Integration (Facility Models)

- **[SNL]** All Milestones have been completed on time.
- **[LLNL]** This project ended at the end of the fiscal year. This project did not have any specific deliverables for the year, but all activities and tasks have been completed. Results from this year's calculations have been provided to SNL.

MIP Monitor and CoDCon

- **[PNNL]** PNNL submitted the final annual report for the MIP monitor effort. Information was gathered and presented from authors from PNNL, University of Tennessee-Knoxville, University of Texas-Austin,
- **[SRS, SRNL]** The project will be conducting close out actions for the upcoming months.

EXPLORATORY RESEARCH / FIELD TESTS

Microcalorimetry

- **[LANL]** Completed high-bandwidth array readout demonstration and submitted report describing the results. We developed a cryogenic system capable of operating over 2000 microcalorimeter detector elements, and implemented a scalable system of readout electronics that supports 128 channels per module. This demonstration has shown key capabilities needed to operate microcalorimeter gamma detector arrays on the 1000-pixel scale needed to give comparable throughput to high-purity germanium detectors, and represents a major step towards a practical analytical instrument.

In situ Measurement of Pu Content in U/TRU Ingot

- **[INL]** Completed the M3 report, NTRD-MPACT-2017-000247, and delivered to NTD and CAM.

H-Canyon Support

- **[SRNL]** PNNL researcher Dave Meier made a final visit to close out the project and return equipment.

For more information on MPACT contact Mike Miller at (208) 526-2813.

Fuel Cycle Options Campaign

CAMPAIGN MANAGEMENT

- **[ANL, INL]** Approved all the FY 2018 Work Packages (Rev. 0) for the Campaign lab teams.
- **[INL, ANL]** Continued the planning for the Campaign meeting of October 17-18, by finalizing the meeting Agenda and ensuring that all the required access requests for DOE-Nevada are being processed.

EQUILIBRIUM SYSTEM PERFORMANCE (ESP)

Equilibrium System Analyses

- **[ANL, BNL, INL, ORNL]** Submitted the level 3 milestone report entitled "Report on Fuel Cycle Concepts – FY 2017 Update" by T. K. Kim, et al. This report is a deliverable under the Work Package "FT–17AN12010201 – Equilibrium System Performance (ESP) - ANL." The Fuel Cycle Options campaign has been collecting information on nuclear fuel cycles that are currently under development and has assessed the claimed fuel cycle performance characteristics. In this study, the information on additional 15 fuel cycles was collected and summarized using the template developed by the FCO campaign. The 15 fuel cycles include fuel cycles utilizing 11 innovative fuel and advanced reactor concepts, and 4 foreign national fuel cycle concepts. In this study, it was concluded that the claimed fuel cycle performance characteristics of the 15 fuel cycles are consistent with the findings in the E&S study.
- **[INL]** INL's FY17 activities on the analyses of alternative options for EG29 and EG30 were documented on the report titled, H. Hiruta and B. Dixon, "INL's analyses of alternative options for the most promising two-stage equilibrium fuel cycle systems", which is currently under review
- **[ANL, BNL, INL, ORNL]** Presented the following paper at the GLOBAL 2017 conference in Seoul, Republic of Korea, September 24 -29, 2017:
  - T. K. Kim et al., "Assessment of Fuel Cycle Characteristics of Advanced Nuclear Energy Systems."
- **[ORNL]** Reviewed draft FY18 Work Package descriptions for the FCO Campaign and provided feedback to campaign leadership regarding tasks descriptions, individuals/labs involved, and budgets.
- **[ORNL]** Ben Betzler traveled to the GLOBAL 2017 Fuel Cycle Conference in Seoul, Korea, and presented on behalf of the Campaign the paper "Fuel Cycle Analysis of Thermal and Fast Spectrum Molten Salt Reactors". Ben attended technical and plenary sessions, and networked with collaborators from other national laboratories, and looked for opportunities to contribute ideas to the future Campaign activities.
- **[ORNL]** ORNL contributed to ANL's DOE Level 3 milestone report by evaluating four types of fuel cycles: (1) the Advanced Fuel CANDU Reactor, (2) UK Open vs. Closed Fuel Cycle, (3) CONVERT, and (4) TOP-MOX. A summary of each of these fuel cycles were provided and the fuel cycles were categorized into one or more evaluation groups as identified in the Evaluation and Screening Study, and identified any claimed impacts on the fuel cycle performance and resolved any inconsistent claims with the findings in the Evaluation and Screening report. Review and comments were provided on this report.

Economics and Financial Risk Assessment

- **[ANL, INL]** Submitted the level 3 milestone report entitled "Report on Cost Estimation Algorithm for Advanced Nuclear Reactors" by F. Ganda, et al. This report is a deliverable under the Work Package "FT–17AN12010201 – Equilibrium System Performance (ESP) - ANL." The report describes the development of an algorithm for estimating the capital cost of any nuclear reactor design, and provides an example of its application to the construction cost estimation of an advanced reactor concept. The developed approach provides an efficient, transparent and defensible framework for estimating the expected construction costs of different reactor designs. The approach can be scaled based: (1) on the fidelity with which the cost of a particular reactor design needs to be known, and the associated resources that are planned to be expended on such efforts; and (2) on the amount of details available for a particular reactor design, which in turn will generally depend on the maturity of each concept.
- **[ANL, INL]** Submitted the level 3 milestone report entitled "Advanced Fuel Cycle Cost Basis - 20-17 Edition" and has been placed on the FCO SharePoint site in the "Documents and Reports" area in a folder titled "Cost Basis 2017 Report files". This completes milestone M3FT-17IN120102033, "Report on Updated Sections of the Fuel Cycle Cost Basis Report" in work package FT-17IN12010203, "Equilibrium System Performance (ESP) - INL". This is a full edition of the Cost Basis Report that will be sent through the process for external release to meet a February, 2018 milestone. The files include a main report, a folder with the module files and another folder with supporting documents. The main report includes several new sections or revisions to existing sections, with the most significant addition being a new chapter documenting the primary methods used for cost estimating. This is a first step in overhauling the entire report over time and module by module with a more rigorous estimating approach. Major revisions to several modules were performed, including the LWR and SFR modules and the electrochemical reprocessing/remote fabrication module. The market price-based front-end modules were augmented with an additional method for projecting future price ranges based on historic data. All modules were updated to include new front matter that informs on the estimation methods used, the escalation factors, change history, and potential information to include in future major updates.
- **[ANL]** Finalized the F2/D2 module (on pyro-processing and remote fabrication) for the Cost Basis Report milestone due at the end of September. The F2/D2 module was sent to Dr. Mark Williamson (ANL) for his comments and revisions.
- **[INL]** Added new content with a uranium price forecast and forecast for the market for enrichment into the Cost Basis Report. Based on historical data, the analyses generate price forecasts for uranium and enrichment. Coupled with the causal forecasts in the CBR, the two methods provide a solid basis for price expectations in economic analysis of the nuclear fuel cycle. In addition to the price forecast analysis, Hansen reviewed many of the modules as part of the Cost Basis Report update.

Maintenance of Fuel Cycle Catalog

- **[SNL]** Sandia upgraded the platform for the Public Nuclear Fuel Cycle Options Catalog from SharePoint 2010 to SharePoint 2013 on September 29, 2017. The transition went smoothly and, because the necessary changes had been made, there was no interruption of service or format on the public Nuclear Fuel Cycle Options Catalog. In addition, a user made us aware of some document links that were not working properly; non-functioning links were identified and repaired.

DEVELOPMENT, DEPLOYMENT AND IMPLEMENTATION ISSUES (DDII)

Technology and System Readiness

- **[BNL, INL, ANL]** Submitted the level 3 milestone report entitled “Lessons Learned from Trial Application of the TSRA Process to Example Metallic Fuel and Aqueous Reprocessing Systems” by M. Todosow, et al. This report is a deliverable under the Work Package “FT-17BN12010302 Rev 2 – Development, Deployment, and Implementation Issues (DDII) - BNL.” Based on the FCT QA procedure for QRL-3 reports, Dr. A. Cuadra reviewed the document.
- **[INL]** Continuing work on the technology and system readiness analysis of the aqueous recycle portion of the fuel cycle for the Materials Recovery and Waste Form Development campaign. Contributed to the report titled “Lessons Learned from Trial Application of the TSRA Process to Example Metallic Fuel and Aqueous Reprocessing Systems”. Separations subsystem. Finished addressing comments received on the Fuel Chopping and Leaching Subsystem from two technical reviewers. Started development of a structure for the technology development roadmap portion of the TSRA process.

Transition to Alternative Fuel Cycle

- **[INL, ANL]** Submitted the level 3 milestone report entitled "Summary Analysis Report on Transition to a Second Generation Nuclear Fuel Cycle", this completes milestone M3FT-17IN120103031, "Report providing the summary of fuel cycle transition to the most promising options" in work package FT-17IN12010303, "Development, Deployment, and Implementation Issues (DDII) - INL". This report summarizes the body of analyses completed over the last few years for transitioning to the "most promising" fuel cycles identified in the Evaluation and Screening report. The document is shorter and written at a higher level than previous reports on this topic to make the work available to a broader audience while also providing a more strategic perspective for the work.
- **[ANL]** Assisted in writing of the INL’s M3 report of “Report Providing the Summary of Fuel Cycle Transition to the Most Promising Options”, providing the summary of fuel cycle transition to the most promising options. New figures and tables were created to facilitate communication of results.
- **[ANL]** Presented the following papers at the GLOBAL 2017 conference in Seoul, Republic of Korea, September 24 -29, 2017:
  - E. Hoffman, al., “Evaluation of a Closed Fuel Cycles Using Fast and Thermal Reactors.”
  - B. Feng, et al., “Transition to a Fast and Thermal Recycle Fuel Cycle with LEU Startup.”
- **[LLNL]** Informal review of year-end deliverables as requested.
- **[ORNL]** Reviewed draft FY18 Work Package descriptions for the FCO Campaign and provided feedback to campaign leadership regarding tasks descriptions, individuals/labs involved, and budgets.
- **[ORNL]** ORNL gave a presentation at the international SCALE workshop on how COUPLE/ORIGEN/OPUS has been used to generate cross section and recipes for use in ORION and now how the ORIGEN-API is now incorporated into ORION. This was to raise the awareness of the application of inventory codes to support fuel cycle assessment, and the importance of using robust methods to do so.
- **[ORNL]** Slides have been produced for presentation at the Campaign annual meeting in Las Vegas in October.
- **[ORNL]** The cross sections and multiple recipes for LWR and LWR to MOX fuel cycle models have been generated for evaluation of the impact in ORION. Both the cross sections and recipes were used to determine the differences between fuel cycle metrics such as radioactivity at 100 and 100k years, U

and Pu radionuclide inventories, and multi-reactor support ratios. This is in support of FY18 activities.

Transition Economics

- **[INL]** Worked with INL collaborators to set up alternative EG-23/24 No-growth scenarios in VISION for examining economics impacts of delaying facility builds to increase utilization.
- **[INL]** Worked with INL collaborators and developed a model to evaluate alternative build profiles for the deployment of separations facilities and fuel fabrication. The analysis supports economic comparison of alternative transition possibilities. This analysis is preliminary to a more in-depth economic analysis in FY18 on fuel cycle transition options.

Regional and Global Impacts

- **[INL, BNL, PNNL]** As reported in August, delivered the level 2 milestone report on August 31, "Market Penetration of Nuclear Power under Various Technology and Climate Change Policy Scenarios" by Sonny Kim, Arantxa Cuadra-Gascon, and Brent Dixon. This report completed the Level 2 milestone, M2FT-17IN120103033 in work package FT-17IN12010303, "Development, Deployment and Implementation Issues (DDII) – INL", due September 1st, 2017. The report summarized the body of work to date conducted to investigate the current and future role of nuclear energy in the context of the evolving US regional and global energy system, including examining the regional and global impact to nuclear energy of clean energy scenarios and availability of CCS, renewable and energy storage technologies. Focus on nuclear energy issues include sensitivity assessments of nuclear capital costs, lifetime extensions and nuclear energy deployment and availability, traditional and non-traditional role of nuclear energy, lifecycle analysis of the nuclear energy systems, and assessment of alternative nuclear fuel cycle and reactor technologies.
- **[PNNL]** Prepared for fiscal year transition and assessed research needs for FY18 regarding nuclear energy use and deployment within the context of evolving regional and global energy systems. Participated in weekly teleconferences.

For more information on Fuel Cycle Options contact Temitope Taiwo (630) 252-1387.

Joint Fuel Cycle Study Activities

JFCS Oversight

- Research of critical technology aspects to support the Integrated Recycling Test (IRT) continues. Campaign personnel continue to operate and test equipment with irradiated fuel to acquire data to support assessments of technical and economic feasibility and nonproliferation acceptability of electrochemical recycling.
- Processing of the second batch of FFTF MOX in the IRT electrorefiner and subsequent distillation operations were completed in September.
- Close coordination is occurring with MFC Analytical Laboratory to receive analysis results from critical samples to enable critical path operations. Approximately 85 processing samples from irradiated operations have been delivered to MFC Analytical Laboratory

Electrochemical Recycling Activities

Head-End

- In September, head-end equipment was moved to storage after completing refurbishing and equipment updates the for use with light water reactor fuel.

Oxide Reduction System

- The oxide reduction system was held in hot standby during September pending additional process experiments. The second of two electro-reduction experiments was previously completed in June.

Electrorefiner System

- The processing of the MOX2 batch in the Electrorefiner was completed in September. A method was developed to size uranium cathode product into small enough pieces to be placed in universal basket for LCC operations. Phase II qualification of the liquid cadmium cathode equipment (for U/TRU recovery) was completed in September. Phase III (in-cell) qualification the liquid cadmium cathode equipment began in September and is scheduled for completion in October.

Remote Distillation Systems

- The remote distillation system was used to separate salt from the second MOX batch from the electrorefiner system in September. Additionally, components to be used in U/TRU recovery were exposed to heat cycle testing in the remote distillation system.

JFCS Critical Gap Research and Development

- **[INL]** Method development for cadmium and salt distillation process continued in the prototype distillation apparatus at the Engineering Development Laboratory. Experiments with alternative crucible materials are ongoing. Efforts in this area are focused on alternatives to BeO crucibles destined for use in electrorefining, distillation, and casting systems.
- **[PNNL]** In September, work was performed to summarize sodalite synthesis and drafted into manuscript to be submitted for publication later this year. JFCS Fuels

Fuels – IRT

- In September, the casting/sampling furnace management self-assessment was completed. Additionally, several casting runs were successfully performed with uranium and zirconium in the casting/sampling furnace.

Fuels – Critical Gap

- FCCI diffusion couple testing continued in September. Samples were prepared and awaiting analysis via electron microscopy.

For more information on Joint Fuel Cycle Studies Activities contact Mike Goff (208) 526-1999 or Ken Marsden (208) 533-7864.

Program Assessment & Coordination

PROGRAM MANAGEMENT

- Working with OSTI acknowledgement process.
- Coordinated, hosted, and facilitated NE customer meetings.
- Supported efforts to finalize FY18 WP's.

QUALITY SUPPORT

- **[ANL]** Completed and submitted surveillance report milestone. Organized July visit by QA Manager.
- **[BNL]** Participated in QAPOC conference call. Assisted WP manager in submitting milestone deliverables.
- **[INL]** NTRD QA Comprehensive report completed and approved. The report is located in PICS and the INL document management system.
- **[LANL]** Participated in biweekly conference calls, refined FY18 work package information, working on LANL WP reviews.
- **[ORNL]** Reviewed numerous milestone submissions for September to ensure that applicable FC QA requirements were met. No problems were identified.
- **[PNNL]** Reviewed the final Project Review of Argonne National Laboratory at the request of the DOE NTRD QA Manager. Meeting with NTRD work package managers to review and verify that the appropriate QA grading is identified in FY2018 NTRD work packages.
- **[SRNL]** SRNL continue to participate in biweekly conference call, answer emails and submitted FY18 work package.

COMMUNICATIONS

- Provided final copy of GLOBAL2019/Top Fuel2019 teaser video for GLOBAL2017 showing
- Received facility virtual tours to support outreach activities.

INFORMATION MANAGEMENT

- The Documentum D2 interface software has been upgraded to version 4.7.

REACTOR DIGITIZATION

- Work was completed and the level 2 milestone was uploaded into PICS on 9/28/17.

For more information on Program Assessment and Coordination contact Bonnie Hong (208) 526-0629.

AFCI-HQ Program Support

UNIVERSITY PROGRAMS

Site: University Research Alliance at West Texas A&M University in Canyon TX, and the following universities: University of Michigan, University of Tennessee, University of California at Berkeley, Massachusetts Institute of Technology, University of Utah, Rensselaer Polytechnic Institute, Washington State University, Colorado School of Mines, University of Nevada at Las Vegas, Clemson University, University of South Carolina, Purdue University, and other universities.

Universities engaged in Nuclear Technology research via URA programs since 2001:

Boise State University
Boston College
Clemson University
Colorado School of Mines
Georgia Institute of Technology
Idaho State University
Florida State University
Kansas State University
Massachusetts Institute of Technology
Missouri University of Science and Technology
North Carolina State University
Northern Illinois University
Northwestern University
Ohio State University
Pennsylvania State University
Purdue University
Rensselaer Polytechnic Institute
Rutgers University
Texas A&M University
University of Arkansas
University of California at Berkeley
University of California at Santa Barbara
University of Chicago
University of Cincinnati
University of Florida
University of Idaho
University of Illinois at Urbana-Champaign
University of Michigan
University of Missouri
University of Nevada at Las Vegas
University of New Mexico
University of North Texas
University of Notre Dame
University of Ohio
University of South Carolina
University of Tennessee at Knoxville
University of Texas at Austin
University of Virginia
University of Wisconsin
Vanderbilt University
Virginia Commonwealth University
Washington State University

INNOVATIONS IN NUCLEAR TECHNOLOGY R&D AWARDS (FORMERLY INNOVATIONS IN FUEL CYCLE RESEARCH AWARDS)

Summary Report

- University Research Alliance provided information to the 2017 First Place winners of the Open Competition and worked with the American Nuclear Society on the Innovations in Nuclear Technology R&D Awards student session, to be held Thursday November 2 at the American Nuclear Society Winter Meeting in Washington DC.
- University Research Alliance ordered desktop awards for the 2017 award winning students.
- University Research Alliance continued to improve the email distribution list in preparation for the 2018 Innovations Awards.

For more information on the University Research Alliance contact Cathy Dixon (806) 651-3401.